

TITLE: Effect of a Frequency Perturbation in a Chain of Syntonized Transparent  
Clocks

---

WORKING ITEM: Transparent Clocks  
Revision: 1

---

AUTHOR(S): Geoffrey M. Garner

---

SOURCE(s) / CONTACT(s): Geoffrey M. Garner (E-mail: [gmgarner@comcast.net](mailto:gmgarner@comcast.net) )  
Tel. +1 732 758 0335

---

DATE: March 10, 2007

---

## Abstract

This contribution analyzes the propagation of error in syntonized frequency in a chain of syntonized transparent clocks due to a sinusoidal frequency perturbation at the first clock downstream from the master clock. It is shown that if residence time is much less than frequency update interval a very large number of hops is required before the effect of a frequency offset perturbation on downstream accumulates to the level of the perturbation (e.g., for residence time on the order of 0.001 of the frequency update interval, the frequency offset amplitude due to the applied perturbation after 100 hops is 0.2% of the applied perturbation amplitude). For AVB networks, where residence time could be as large as one-tenth the frequency update interval, the frequency offset accumulates to the level of the perturbation after 11 hops. After 7 hops, the frequency offset is approximately half the level of the applied perturbation. The phase offset also accumulates slowly when residence time is small compared to frequency update interval, though the accumulation is faster than for the frequency offset accumulation (e.g., for residence time on the order of 0.001 of the frequency update interval, the phase offset amplitude due to the applied perturbation after 100 hops is 0.21 of the applied perturbation amplitude). For AVB networks, where residence time could be as large as one-tenth the frequency update interval, the phase accumulation is about twice the applied perturbation amplitude after 7 hops. A scheme (see [8]) that does not syntonize the TCs but uses the measured frequency offset relative to the master to adjust the phase was also investigated. Here, the phase accumulation due to a sinusoidal phase perturbation is slower than in the syntonized chain case, though the results are almost indistinguishable for small ratios of residence time to frequency update interval, even for a very large number of hops (e.g., for residence time on the order of 0.001 of the frequency update interval, the phase offset amplitude due to the applied perturbation after 100 hops is 0.2 of the applied perturbation amplitude). For AVB networks, where residence time could be as large as one-tenth the frequency update interval, the phase accumulation is about 1.2 times the applied perturbation amplitude after 7 hops.

This contribution also suggests that if 802.1AS networks must tolerate sinusoidal phase wander in the clocks, consideration should be given to the level of wander that must be tolerated and the desired performance. The examples here used 100 ns sinusoidal wander amplitude; this was taken from [6], but no justification was given (either in [6] or here) for this level. It should be noted

that the phase error accumulation results in section 4 are unfiltered; section 5 shows an example of the reduction that results after endpoint filtering.

## 1 Introduction

Recent discussion on the P1588 reflector [1], [2] has raised concerns that a chain of syntonized transparent clocks may exhibit excessive jitter amplification and accumulation due to gain peaking. Specifically, it is stated in [1] that the jitter accumulation may be excessive when the period of a frequency perturbation is on the order of twice the frequency measurement interval. It is added in [2] that the accumulation occurs due to effective gain peaking in the syntonization mechanism.

It is well-known that large jitter and wander accumulation in a chain of phase-locked loops may occur due to excessive gain peaking. This effect was analyzed in [3] for the case of a chain of digital regenerators. The transfer function and frequency response for such a chain was computed, and the frequency response was integrated analytically to obtain the mean-square jitter as a function of bandwidth and gain peaking (the integration was necessary because the jitter generation was a random process). The regenerator model of [3] was linear, second-order with 40 dB/decade roll-off; this model reflected the regenerators commonly used in PDH telecommunications networks at the time. The effect was subsequently analyzed for SDH, SONET, and OTN networks for phase-locked-loop (PLL) based regenerators, using linear, second-order models with 20 dB/decade roll-off. The analysis for OTN is documented in [4]. This analysis uses the same techniques as that in [3], i.e., the frequency response for the chain of second-order, linear filters is computed and integrated over frequency to obtain mean-square jitter. The analysis of [4] shows that, with 0.1 dB of gain peaking, the jitter network limits for PDH, SDH/SONET, and OTN are met for a chain of 50 regenerators (the OTN regenerator hypothetical reference model consists of a chain of 50 regenerators; see Appendix III of [4]). The analysis assumes that the regenerators also meet the respective jitter transfer and generation requirements given in [4]. As a result of the analyses of [3] and [4] and other similar analyses, the gain peaking for regenerators and clocks used in telecommunications networks is limited to 0.1 dB.

The analyses of [3] and [4] assume a chain of 2nd order PLLs, with either 40 dB/decade roll-off [3] or 20 dB/decade roll-off [4]. Such PLLs have inherent gain peaking. However, the syntonization process for a transparent clock (TC) described in section 12.1.2 of [5] is not a second-order PLL. In particular, there is no apparent gain peaking present in the syntonization process. In addition, the quantity of interest in a chain of TCs is the frequency offset relative to the master clock at the beginning of the chain, and how this frequency offset varies with the number of hops. The primary uses of this frequency are for measurement of residence time and link propagation time. The purpose of the present contribution is to explicitly evaluate the accumulation of frequency offset error, if any, that occurs in a chain of syntonized TCs.

The contribution is organized as follows. A difference equation for the frequency offset relative to the master clock is derived in section 2. This is actually a partial difference equation, i.e., its independent variables are discrete time index and hop number index. The stability of this equation as a function of hop number is considered in section 3. Section 4 analyzes unfiltered phase error accumulation. Section 6 discusses wander tolerance, and shows some example results for filtered phase error accumulation. Conclusions are given in section 7. References are contained in section 8.

## 2 Transfer function for the syntonization of a TC

Consider a chain of TCs timed by a master at the beginning of the chain. The master is labeled node 0, and the TCs are labeled nodes 1 through  $N$ , respectively. We assume each TC performs a

frequency update every  $M^{\text{th}}$  synch interval on receipt of the Sync and Follow\_Up message for that synch interval, and that the frequency update is done before the measurement of residence time (i.e., residence time is measured using the new frequency rather than the old). We assume the master frequency is perfect, and neglect phase measurement granularity. Define the following notation:

$i$  = index of Sync message sent for which a frequency update is performed (if a frequency update is performed every  $M$  Synch messages, then this is actually the  $Mi^{\text{th}}$  Sync message; Sync messages for which no frequency update is performed need not be considered in this analysis). The first Sync message is labeled  $i = 0$ .

$k$  = index of node number. The master clock at the beginning of the chain is labeled  $k = 0$ ; the TCs are labeled  $1, 2, \dots, N$ . Note that this scheme differs from the numbering in [6], where the GM is node 1 and the first TC is node 2. Figure 1 below illustrates the two numbering schemes.

$v_{k,i}$  = actual frequency offset of TC  $k$  relative to the master clock, during the frequency update interval between the  $i^{\text{th}}$  and  $(i+1)^{\text{st}}$  Sync messages

$\mu_{k,i}$  = measured frequency offset of TC  $k$  relative to the master clock, when the  $i^{\text{th}}$  Sync and Follow\_Up messages arrive. Note that if the measurement process were perfect, then the measured value would be equal to the actual frequency offset during the previous frequency update interval, i.e.,  $\mu_{k,i} = v_{k,i}$ . However, in general the measurement process is imperfect and this is not true.

$r_{k,i}$  = measured residence time of Sync message  $i$  at TC  $k$ . Note that this will differ from ideal residence time, relative to the master clock, due to the frequency offset of TC  $k$ .

$T_r$  = ideal residence time, relative to the perfect master.

$T_I$  = frequency update interval, relative to the perfect master.

$m_{k,i}$  = corrected master time at TC  $k$  when  $i^{\text{th}}$  Sync message is received (i.e., corrected for the residence times of TCs  $1, 2, \dots, k-1$ ). Note that  $m_{0,i}$  is the time the  $i^{\text{th}}$  Sync message is actually sent, relative to the master clock.

#### Node Numbering conventions (initial node is GM, followed by TCs)

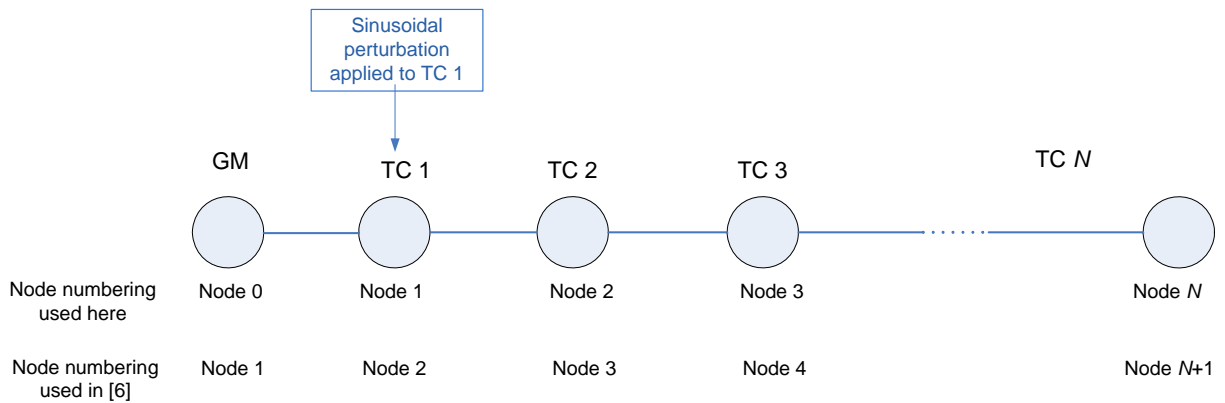


Figure 1. Illustration of node numbering conventions here and in reference [6].

The corrected master time is related to the time the Sync message is sent by the master clock and the residence times in the upstream TCs by

$$m_{k,i} = m_{0,i} + \sum_{j=1}^{k-1} r_{j,i} . \quad (2-1)$$

The residence time at TC  $k$  is related to the frequency offset of TC  $k$  by

$$r_{k,i} = (1 + \nu_{k,i}) T_r . \quad (2-2)$$

Note that  $\nu_{k,i}$  appears in Eq. (2-2) rather than  $\nu_{k,i-1}$  because it is assumed the residence time is computed using the updated frequency. Combining Eqs. (2-1) and (2-2) produces

$$m_{k,i} = m_{0,i} + kT_r + T_r \sum_{j=1}^{k-1} \nu_{j,i} . \quad (2-3)$$

The measured frequency offset of TC  $k$  is equal to the ratio of the elapsed local time during a frequency update interval to the elapsed corrected master time during the same frequency update interval, minus one. For the frequency offset measured at the arrival of the  $i^{\text{th}}$  Sync message, this may be written

$$\begin{aligned} \mu_{k,i} &= \frac{T_l(1 + \nu_{k,i-1})}{m_{0,i} + kT_r + T_r \sum_{j=1}^{k-1} \nu_{j,i} - \left[ m_{0,i-1} + kT_r + T_r \sum_{j=1}^{k-1} \nu_{j,i-1} \right]} - 1 \\ &= \frac{T_l(1 + \nu_{k,i-1})}{T_l + T_r \sum_{j=1}^{k-1} (\nu_{j,i} - \nu_{j,i-1})} - 1 \\ &= \frac{T_l \nu_{k,i-1} - T_r \sum_{j=1}^{k-1} (\nu_{j,i} - \nu_{j,i-1})}{T_l + T_r \sum_{j=1}^{k-1} (\nu_{j,i} - \nu_{j,i-1})} . \\ &= \frac{\nu_{k,i-1} - \frac{T_r}{T_l} \sum_{j=1}^{k-1} (\nu_{j,i} - \nu_{j,i-1})}{1 + \frac{T_r}{T_l} \sum_{j=1}^{k-1} (\nu_{j,i} - \nu_{j,i-1})} \end{aligned} \quad (2-4)$$

The frequency is adjusted by reducing the current frequency by an amount equal to the measured frequency offset of the TC relative to the master. Then, the new actual frequency offset is related to the old actual frequency offset by

$$\nu_{k,i} = \nu_{k,i-1} - \mu_{k,i} . \quad (2-5)$$

Inserting Eq. (2-4) into Eq. (2-5) produces

$$\begin{aligned}
v_{k,i} &= v_{k,i-1} - \frac{v_{k,i-1} - \frac{T_r}{T_l} \sum_{j=1}^{k-1} (v_{j,i} - v_{j,i-1})}{1 + \frac{T_r}{T_l} \sum_{j=1}^{k-1} (v_{j,i} - v_{j,i-1})} \\
&= \frac{v_{k,i-1} - v_{k,i-1} + \frac{T_r}{T_l} \sum_{j=1}^{k-1} (v_{j,i} - v_{j,i-1})}{1 + \frac{T_r}{T_l} \sum_{j=1}^{k-1} (v_{j,i} - v_{j,i-1})} + O(v_{k,i}^2) \\
&= \left[ \frac{T_r}{T_l} \sum_{j=1}^{k-1} (v_{j,i} - v_{j,i-1}) \right] \left[ 1 - \frac{T_r}{T_l} \sum_{j=1}^{k-1} (v_{j,i} - v_{j,i-1}) \right] + O(v_{k,i}^2) \\
&= \frac{T_r}{T_l} \sum_{j=1}^{k-1} (v_{j,i} - v_{j,i-1}) + O(v_{k,i}^2)
\end{aligned} \tag{2-6}$$

Now, the frequency offsets are small compared to 1, i.e.,  $|v_{k,i}| \ll 1$ . Then the terms of  $O(v_{k,i}^2)$  are small compared to the terms of  $O(v_{k,i})$ , and Eq. (2-6) may be approximated to first order in  $v_{k,i}$  as

$$v_{k,i} = \frac{T_r}{T_l} \sum_{j=1}^{k-1} (v_{j,i} - v_{j,i-1}). \tag{2-7}$$

Eq. (2-7) holds for  $k \geq 2$ . For  $k > 2$ , it may be converted to a recursive form by rewriting it for index  $k-1$  and subtracting the result from Eq. (2-7). The result of this is

$$\begin{aligned}
v_{k,i} - v_{k-1,i} &= \frac{T_r}{T_l} \sum_{j=1}^{k-1} (v_{j,i} - v_{j,i-1}) - \frac{T_r}{T_l} \sum_{j=1}^{k-2} (v_{j,i} - v_{j,i-1}) \\
&= \frac{T_r}{T_l} (v_{k-1,i} - v_{k-1,i-1}) \quad k > 2
\end{aligned} \tag{2-8}$$

An equation for  $k = 2$  is obtained by simply substituting  $k = 2$  in Eq. (2-7). Then, Eq. (2-7) is equivalent to

$$\begin{aligned}
v_{2,i} &= \frac{T_r}{T_l} (v_{1,i} - v_{1,i-1}) \\
v_{k,i} &= v_{k-1,i} \left( 1 + \frac{T_r}{T_l} \right) - \frac{T_r}{T_l} v_{k-1,i-1} \quad k > 2
\end{aligned} \tag{2-9}$$

### 3 Stability analysis for variation of frequency offset as a function of number of hops

We are interested in how a small frequency perturbation applied at the first TC downstream from the master ( $k = 1$ ) propagates through the successive TC. The master frequency is assumed perfect. Then, we set

$$\begin{aligned} v_{0,i} &= 0 \\ v_{1,i} &= Ae^{j\omega i} \end{aligned} \quad (3-1)$$

where  $\omega$  is the discrete frequency,  $A$  is the amplitude of the perturbation, and  $j = \sqrt{-1}$  (i.e., in this section we do not use  $j$  as an index). The first of Eq. (2-9) may be rewritten

$$v_{2,i} = A \frac{T_r}{T_l} e^{j\omega i} (1 - e^{-j\omega}). \quad (3-2)$$

As expected for linear systems,  $v_{2,i}$  is equal to  $v_{1,i}$  multiplied by a complex frequency response  $H_1(e^{j\omega})$ . This means that the resulting frequency offset at any TC is sinusoidal with a respective phase (as expected), and we may use the second of Eq. (2-9) to compute the frequency response between TCs  $k$  and  $k+1$ . To do this, take the  $z$ -transform of the second of Eq. (2-9) and then set  $z = e^{j\omega}$ . Taking the  $z$ -transform produces

$$N_k(z) = N_{k-1}(z) \left( 1 + \frac{T_r}{T_l} - \frac{T_r}{T_l} z^{-1} \right), \quad (3-3)$$

where  $N_k(z)$  is the  $z$ -transform of  $v_{k,i}$ , and the result for the  $z$ -transform of a shifted sequence has been used (i.e., the the  $z$ -transform of a sequence obtained by replacing the index by the index minus one is equal to  $z^{-1}$  multiplied by the  $z$ -transform of the unshifted sequence). The complex frequency response between TCs  $k-1$  and  $k$ , with  $k \geq 3$ , is

$$H(e^{j\omega}) = 1 + \frac{T_r}{T_l} - \frac{T_r}{T_l} e^{-j\omega}. \quad (3-4)$$

The frequency response at TC  $k$  is obtained by multiplying Eq. (3-2) by Eq. (3-4) raised to the  $k-2$  power (the power is  $k-2$  because, in getting from TC 2 to TC  $k$ ,  $k-2$  hops are traversed). The result is

$$v_{k,i} = A \frac{T_r}{T_l} e^{j\omega i} (1 - e^{-j\omega}) \left( 1 + \frac{T_r}{T_l} - \frac{T_r}{T_l} e^{-j\omega} \right)^{k-2}. \quad (3-5)$$

The amplitude of the response may be obtained, as a function of frequency, by computing the complex amplitude of Eq. (3-5). This is done omitting the constant  $A$  as that is the amplitude of the input perturbation (and what is of interest here is how the perturbation grows or decays with the number of hops). The result is

$$\left| N_k(e^{j\omega}) \right|^2 = \left( \frac{T_r}{T_l} \right)^2 [2(1 - \cos \omega)] \left[ 1 + \frac{2T_r}{T_l} \left( 1 + \frac{T_r}{T_l} \right) (1 - \cos \omega) \right]^{k-2} \quad k \geq 2, \quad (3-6)$$

where  $N_k(e^{j\omega})$  is the frequency response between the input perturbation and TC  $k$ . In obtaining Eq. (3-6), we used the results

$$\left| 1 - e^{j\omega N} \right|^2 = (1 - \cos \omega N)^2 + \sin^2 \omega N = 2(1 - \cos \omega N) \quad (3-7)$$

and

$$\begin{aligned}
|1 + b - be^{-j\omega}|^2 &= |1 + b - b \cos \omega + jb \sin \omega|^2 \\
&= (1 + b - b \cos \omega)^2 + b^2 \sin^2 \omega \\
&= (1 + b)^2 - 2b(1 + b) \cos \omega + b^2 \\
&= 1 + 2b + 2b^2 - 2b(1 + b) \cos \omega \\
&= 1 + 2b(1 + b)(1 - \cos \omega)
\end{aligned} \tag{3-8}$$

The minimum value of the frequency response, Eq. (3-6), is zero, and occurs at zero frequency. The maximum value occurs at odd multiples of  $\pi$  (recall that  $\omega$  is the discrete frequency). The maximum value is

$$\begin{aligned}
|N_k(e^{j\omega})|_{\max}^2 &= 4 \left( \frac{T_r}{T_I} \right)^2 \left[ 1 + \frac{4T_r}{T_I} \left( 1 + \frac{T_r}{T_I} \right) \right]^{k-2} \quad k \geq 2 \\
&= 4 \left( \frac{T_r}{T_I} \right)^2 \left[ \left( 1 + \frac{2T_r}{T_I} \right)^2 \right]^{k-2}
\end{aligned} \tag{3-9}$$

Then

$$|N_k(e^{j\omega})|_{\max} = 2 \left( \frac{T_r}{T_I} \right) \left[ 1 + \frac{2T_r}{T_I} \right]^{k-2} \quad k \geq 2 \tag{3-10}$$

It is seen from Eq. (3-10) that the magnitude of the worst-case frequency offset accumulation depends on how long the frequency update interval is compared to the residence time. In general IEEE 1588 networks,  $T_r \ll T_I$ , and a large number of hops are required for the worst case amplitude to exceed 1. For example, if  $T_r/T_I = 0.001$ , then the worst case frequency offset amplitude after 100 hops accumulates to be a factor of

$$|N_k(e^{j\omega})|_{\max} = 2(0.001)[1.002]^8 = 0.00203 \quad k = 100$$

In AVB networks, it is planned to hold Sync messages until Follow\_Up messages arrive and, in worst-case, the residence time could be as long as the synch interval. The frequency update interval is likely to be 10 times the synch interval, i.e.,  $T_r/T_I = 0.1$ . For a seven hop network, the worst-case frequency offset accumulates by a factor of

$$|N_k(e^{j\omega})|_{\max} = 2(0.1)[1.2]^5 = 0.498 \quad k = 7$$

For 10 hops, the result is

$$|N_k(e^{j\omega})|_{\max} = 2(0.1)[1.2]^8 = 0.86 \quad k = 10$$

For 11 hops, the result is

$$|N_k(e^{j\omega})|_{\max} = 2(0.1)[1.2]^9 = 1.03 \quad k = 11$$

It is seen that the frequency offset at successive nodes does not accumulate to the magnitude of the initial perturbation until the 11<sup>th</sup> hop.

The factor by which the frequency offset amplitude accumulates, as a function of TC number, is plotted in Figure 2 for several ratios of residence time to frequency update interval. Note that the horizontal axis starts at TC 2 because the perturbation is applied at TC 1. It is seen that, for ratios of residence time to frequency update interval of 0.01 and 0.001, the perturbation has negligible effect. In all cases, the effect of the perturbation is diminished at the succeeding 9 nodes after TC 1 where the perturbation is introduced.

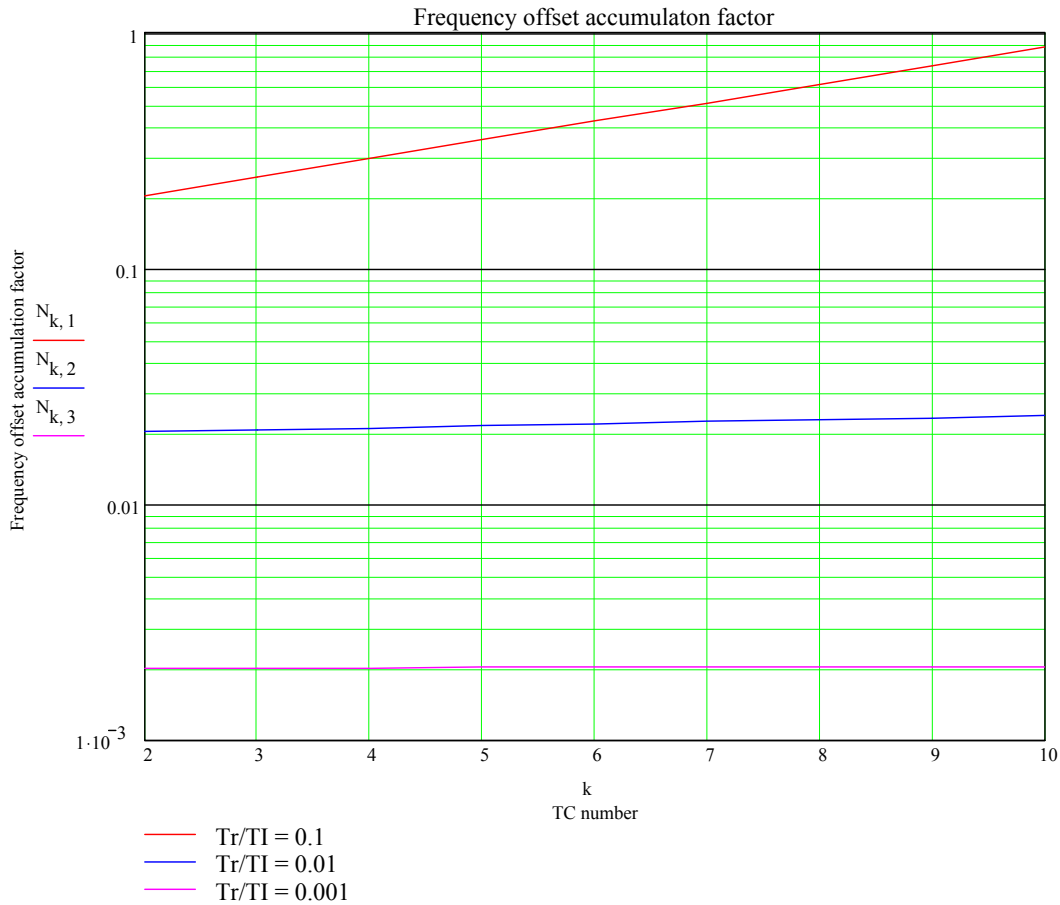


**Figure 2.** Factor by which frequency offset amplitude, due to applied sinusoidal perturbation, accumulates, as a function of TC number, for several ratios  $T_r/T_I$ .

Appendix I contains detailed plots (obtained using Mathcad) of the magnitude of the frequency response (the square root of Eq. (3-6)) as a function of discrete frequency  $\omega$ , for various numbers of hops and ratios of residence time to frequency update interval. The four successive plots are for  $T_r/T_I = 0.001, 0.01, 0.05,$  and  $0.1,$  respectively. Each plot contains results for accumulated frequency offset magnitude at successive nodes (the second subscript,  $k$ , of  $N_{n,k}$ , is the node number minus 1. The final plot shows a maximum frequency response amplitude at  $\omega = \pi$  with amplitude 0.86 for node 10 ( $k = 9$ ), consistent with the above result.

## 4 Unfiltered phase error accumulation over multiple hops

Subsequent to the above analysis, the phase error accumulation was analyzed in [6]. That analysis agreed fundamentally with the results above, but seemed to differ in detail. For example,

[6] stated that both studies indicated that jitter/wander amplification is not server for (1) a long chain of high performance TCs with residence time on the order of 100  $\mu$ s and frequency update interval 0.1 s, and (2) a short chain of AVB TCs, with residence time on the order of 10 ms and frequency update interval 0.1 s. Reference [6] also found that the amplitude growth as a function of number of hops is of the form

$$G = G_0 \left( 1 + a \frac{T_r}{T_l} \right)^n, \quad (4-1)$$

analogous to Eq. (3-10). However, the two studies seemed to differ on details such as worst case frequency update period and specific values of  $G_0$  and  $a$  (see Table 1 of [6]). Part of the difficulty of comparing the results of [6] with the results above is that the results above are for accumulation of frequency offset, while the results in [6] are for accumulation of phase offset. Therefore, it is of interest to extend the above model to obtain phase offset accumulation.

In this section, the results of sections 2 and 3 are used to total phase error accumulation under the assumption that an ordinary clock is collocated with each synchronized transparent clock. We are interested in the component of phase error due to the frequency (or equivalent phase) perturbation applied at the first TC downstream from the master (i.e.,  $k = 1$ ) and the effect of the frequency perturbation at downstream TCs (i.e.,  $k > 1$ ). Now, the phase offset at any TC is computed as the difference between the timestamp of a Sync message when it arrives at that TC and the corrected master egress timestamp for the Sync message. The latter is corrected for measured propagation time on the links upstream from the TC (for the case where the TCs are peer-to-peer) and measured residence time in the upstream TCs. It is seen, therefore, that the accumulated phase error due to the frequency perturbation is equal to the sum of the residence time errors in all the upstream TCs. The residence time error for a single TC is equal to the frequency offset of that TC,  $\nu_{k,i}$ , multiplied by the ideal residence time,  $T_r$ . Then, the accumulated phase error,  $\phi_{m,i}$ , at TC  $m$  at the arrival of the  $i^{th}$  Sync message is

$$\phi_{m,i} = \sum_{k=2}^{m-1} \nu_{k,i} T_r. \quad (4-2)$$

For a sinusoidal frequency perturbation at TC 1 of the form of Eq. (3-1), we may substitute Eq. (3-5) into Eq. (4-2) to obtain the resulting accumulated phase error at TC  $m$ . As in section 3,  $j = \sqrt{-1}$  (i.e., in section 4 we do not use  $j$  as an index). The result is

$$\phi_{m,i} = A \frac{T_r^2}{T_l} (1 - e^{-j\omega}) e^{j\omega t} \sum_{k=2}^{m-1} \left( 1 + \frac{T_r}{T_l} - \frac{T_r}{T_l} e^{-j\omega} \right)^{k-2}. \quad (4-3)$$

Performing the summation produces

$$\begin{aligned}
\phi_{m,i} &= A \frac{T_r^2}{T_I} (1 - e^{-j\omega}) e^{j\omega i} \frac{1 - \left(1 + \frac{T_r}{T_I} - \frac{T_r}{T_I} e^{-j\omega}\right)^{m-2}}{1 - \left(1 + \frac{T_r}{T_I} - \frac{T_r}{T_I} e^{-j\omega}\right)} \\
&= A \frac{T_r^2}{T_I} (1 - e^{-j\omega}) e^{j\omega i} \frac{\left(1 + \frac{T_r}{T_I} - \frac{T_r}{T_I} e^{-j\omega}\right)^{m-2} - 1}{\frac{T_r}{T_I} (1 - e^{-j\omega})} \\
&= AT_r e^{j\omega i} \left[ \left(1 + \frac{T_r}{T_I} - \frac{T_r}{T_I} e^{-j\omega}\right)^{m-2} - 1 \right]
\end{aligned} \tag{4-4}$$

Eq. (4-4) expresses the full sinusoidal response of the phase error. The amplitude of the response is given by

$$|\phi_{m,n}|_{\max} = AT_r \cdot \left[ \left(1 + \frac{T_r}{T_I} - \frac{T_r}{T_I} e^{-j\omega}\right)^{m-2} - 1 \right]. \tag{4-5}$$

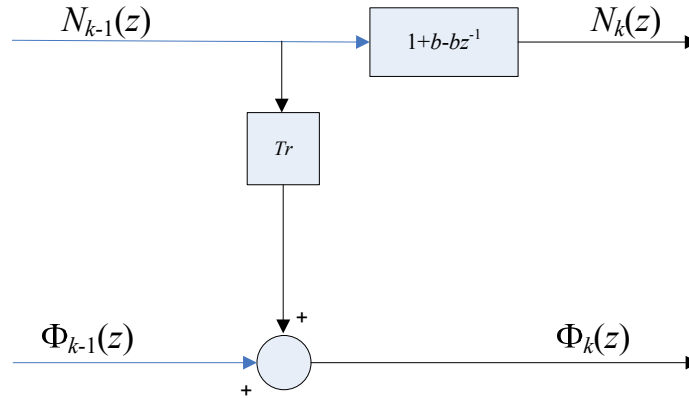
Eq. (4-5) is almost the desired result. The parameter  $A$  in Eq. (4-5) is the frequency offset perturbation amplitude applied at node 1 (the first TC after the master). However, in [6] the input perturbation is expressed as a sinusoidal phase perturbation and not a sinusoidal frequency perturbation. We therefore must express  $A$  in terms of the equivalent sinusoidal phase perturbation. This is easily done by noting that if the frequency offset amplitude at the first TC is  $A$ , the equivalent phase offset amplitude (the quantity testamplitude in the Mathcad file attached to [6]) is  $AT_r$ . In other words, the frequency offset perturbation multiplied by  $T_r$  is equal to the phase perturbation testdeviation in the Mathcad file attached to [6]. The factor of 2 is present because the largest phase perturbation If  $B = AT_r$  is the phase amplitude, then Eq. (4-5) becomes

$$|\phi_{m,n}|_{\max} = B \cdot \left[ \left(1 + \frac{T_r}{T_I} - \frac{T_r}{T_I} e^{-j\omega}\right)^{m-2} - 1 \right]. \tag{4-6}$$

Eq. (4-6) corresponds to the quantity (outputdeviation – testdeviation) in [6]; it is also equal to the quantity residencetime\*(syntonizedrate – 1) in [6]. Essentially, it is the amount that the accumulated phase error exceeds the initial phase error due to the perturbation at the node where it is applied.

Figures 3 and 4 illustrate schematically the accumulation of phase and frequency. They are mathematically equivalent to Eqs. (3-3) and (4-2).

Stages  $k-1 > 1$ , to  $k$   
 (i.e., GM is stage 0 and perturbation is applied at stage 1)



$N_k(z)$  = z-transform of frequency at node  $k$

$\Phi_k(z)$  = z-transform of phase at node  $k$

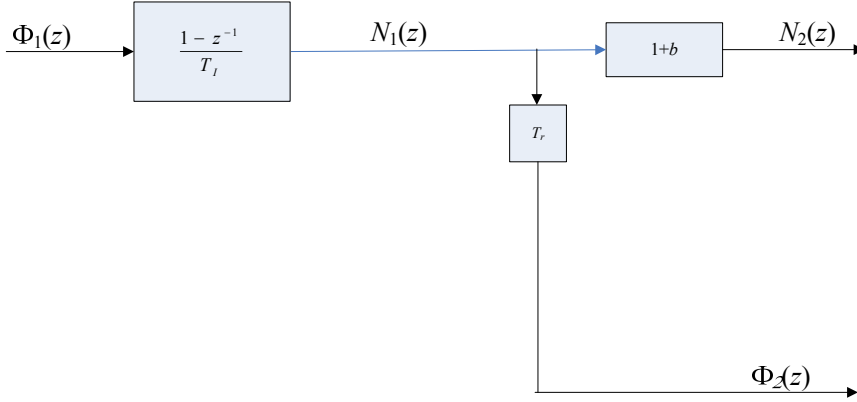
$$b = T_r / T_I$$

$$N_k(z) = (1 + b - bz^{-1})N_{k-1}(z)$$

$$\Phi_k(z) = \Phi_{k-1}(z) + T_r N_k(z)$$

Figure 3. Equivalent block diagram for phase and frequency accumulation difference equations (stages  $k > 2$ ).

Stage 1 to 2  
(i.e., GM is stage 0 and perturbation is applied at stage 1,  
to either frequency  $N_1(z)$  or phase  $\Phi_1(z)$  )



$N_k(z)$  = z-transform of frequency at node  $k$

$\Phi_k(z)$  = z-transform of phase at node  $k$

$$b = T_r / T_I$$

$$N_2(z) = (1 + b)N_1(z)$$

$$N_1(z) = \frac{1 - z^{-1}}{T_I} \Phi_1(z)$$

Figure 4. Equivalent block diagram for phase and frequency accumulation difference equations (stage 2).

Appendix II contains plots, generated using Mathcad, of Eq. (4-6) as a function of discrete frequency, for various numbers of hops and ratios of residence time to frequency update interval. The four successive plots are for  $T_r/T_I = 0.001, 0.01, 0.05,$  and  $0.1,$  respectively. The amplitude of the sinusoidal perturbation is 100 ns, consistent with [6]. Each plot contains results for accumulated phase offset magnitude at successive nodes (the second subscript,  $k,$  of  $\phi_{n,k},$  is the node number minus 1. The plot for  $T_r/T_I = 0.05$  is reproduced in Figure 5 below. The curve for  $n = 1$  (node 2, i.e., the first TC after the TC where the perturbation is applied) shows phase accumulation amplitude of zero. This is because the phase error at this TC is the perturbation itself; we have subtracted that out because we are interested in the accumulation over and above the applied perturbation. The curve for  $n = 2$  (node 3, i.e., the second TC after the TC where the perturbation is applied) shows a phase accumulation amplitude of approximately 20 ns for  $\omega = 2.$  This corresponds to a period of the applied perturbation of approximately  $3.1T_I;$  this is seen by noting that the discrete and continuous frequencies are related by

$$\omega = \Omega T_I = 2\pi T_I / T, \quad (4-7)$$

where  $\Omega$  is the continuous frequency and is equal to  $1/T$ , where  $T$  is the period of the perturbation. Then

$$T = 2\pi T_1 / \omega. \tag{4-8}$$

For  $\omega = 2$ ,  $T/T_1 = \pi \cong 3.1$ . Appendix III reproduces Mathcad results of [6] and adds the computation of (outputdeviation – testdeviation). The result is reproduced in Figure 6 below. In Figure 6, the peak value of (outputdeviation – testdeviation) is approximately 8 ns. In Figure 5, the amplitude of the  $\phi_{n,2}$  curve at  $\omega = 2$  is approximately 8 ns. Figure 7 shows results using the Mathcad file of [6] with the frequency of the applied perturbation equal to  $2.1T_1$  (i.e.,  $\omega$  slightly less than  $\pi$ ). The results show peak value of (outputdeviation – testdeviation) of 1 ns. The amplitude of the  $\phi_{n,2}$  curve in Figure 5 at  $\omega = \pi$  is approximately 10 ns, in agreement.

Table 1 of [6] indicates some other differences between the two studies. The table indicates that the multiplicative factor  $G_0$  is  $2T_1/T_1$  in the study here, while it is 1 in the study there. This difference is due to the fact that the factor cited for the study here is for frequency offset accumulation, and not phase accumulation. The factor  $2T_1/T_1$  is evident in Eq. (3-5), for frequency accumulation (the factor of 2 arises from the maximum absolute value of the factor  $1 - e^{-j\omega}$ ). In Eq. (4-6) here, for phase accumulation, the factor is 1 in agreement with [6]. The value of  $a$  in Table 1 of [6] differs for the two studies because the values are cited for different perturbation periods, i.e.,  $2T_1$  here and  $3T_1$  in [6]. It is not clear why [6] cites the worst case wander as occurring at  $3.1T_1$  and not  $2T_1$ ; Figures 6 and 5 below, which were obtained using the Mathcad listing provided in [6], show larger wander for  $2.1T_1$ . The peaking factors and hops to double in Table 1 of [6] are different for the two studies both because the results are cited at different periods for the perturbation and because one set of results is for frequency offset accumulation and the other phase accumulation. The latter is evident by noting that Eqs. (4-6) for phase accumulation and (3-6) for frequency offset accumulation are different. Our conclusion is that the model here and the model in [6] are consistent.

$$b_{sub 1} = T_{sub r}/T_{sub l} = 0.05$$

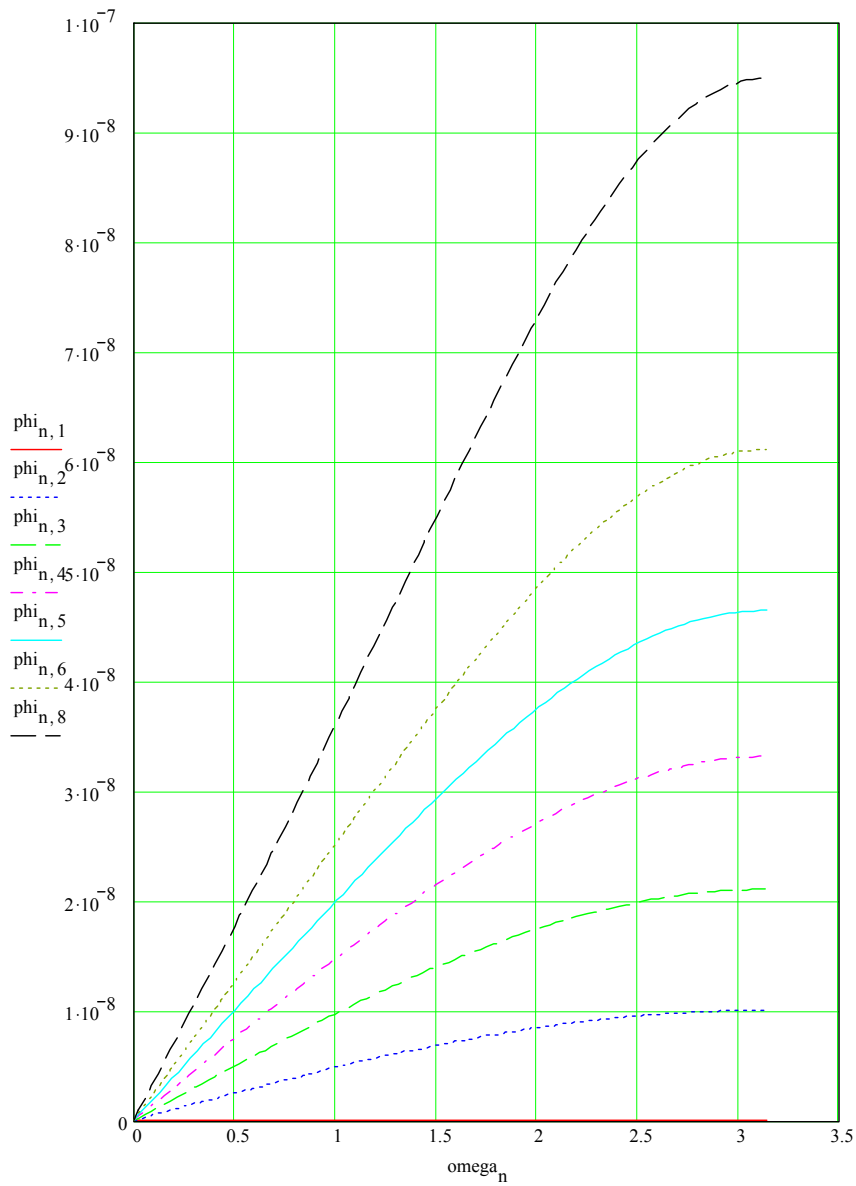


Figure 5. Phase accumulation frequency response magnitude for nodes 2 ( $\phi_{n,1}$ ), 3 ( $\phi_{n,2}$ ), 4 ( $\phi_{n,3}$ ), 5 ( $\phi_{n,4}$ ), 6 ( $\phi_{n,5}$ ), and 10 ( $\phi_{n,9}$ ), respectively, for  $T_r/T_l = 0.05$ .

$T_{sub r}/T_{sub l} = 0.05$

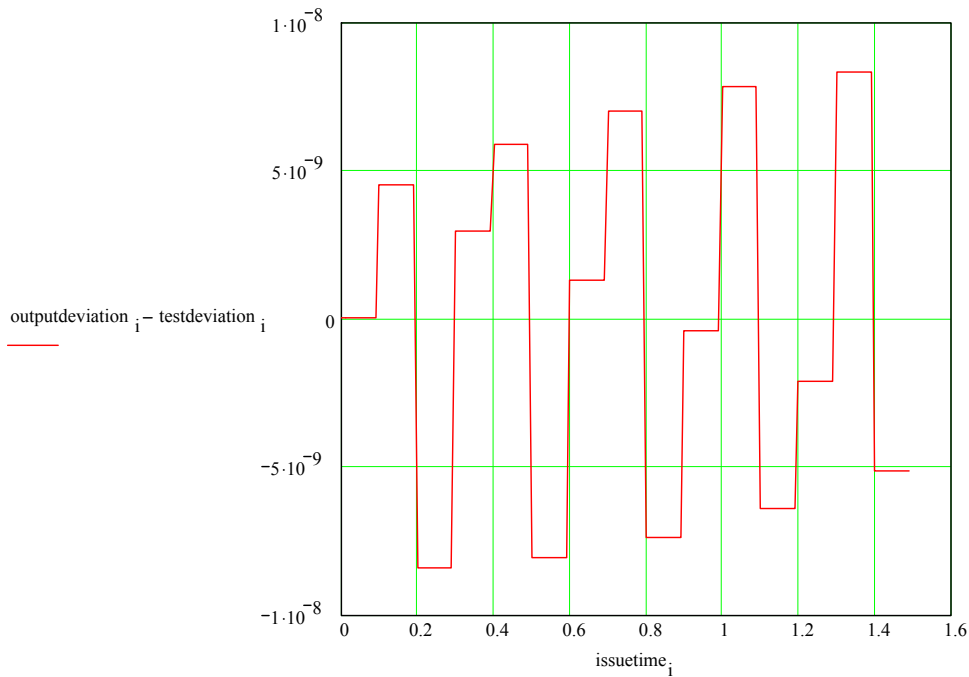


Figure 6. Results for (outputdeviation-testdeviation) using Mathcad file provided in [6]. This quantity is the frequency offset at the first node after the node where the perturbation is applied, multiplied by the ideal residence time. The period of the applied perturbation is  $3.1T_l$ .

$T_{sub r}/T_{sub l} = 0.05$

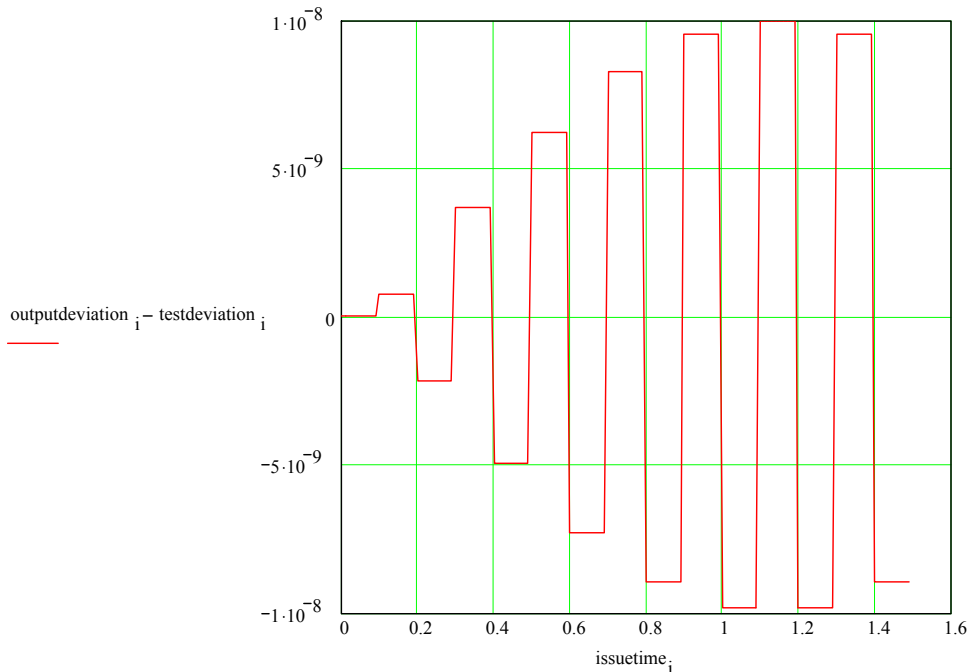


Figure 7. Results for (outputdeviation-testdeviation) using Mathcad file provided in [6]. This quantity is the frequency offset at the first node after the node where the perturbation is applied, multiplied by the ideal residence time. The period of the applied perturbation is  $2.1T_l$ .

## 5 Wander tolerance requirements

The applied sinusoidal perturbation in the previous sections has an amplitude of 100 ns. The amplitude response to this is evaluated for frequencies between 0 and  $0.5/T_I$  (the latter is the Nyquist rate for period  $T_I$ ). The value 100 ns was taken from [6]; however, there is no indication in [6] why this value was chosen. It should be noted that the contribution to clock jitter/wander due to phase measurement granularity is 40 ns. The clock phase noise model used in [7] had noise levels considerably below 100 ns (TDEV for integration times (i.e., observation intervals) less than 0.4 s were less than 1 ns. If it is desired that a synchronization chain in 802.1AS tolerate sinusoidal clock phase wander applied at a node, more consideration should be given to what levels of wander should be tolerated (and what the allowable response should be).

In addition, note that the phase errors computed here are unfiltered; these levels would be reduced by endpoint filtering. For example, Figure 8 shows the results corresponding to Figure 5, but with an endpoint filter with an equivalent 1 s time constant

$$H(z) = \frac{0.1}{1 - 0.9z^{-1}} \quad (5-1)$$

(The equivalent time constant is seen to be 1 s by noting that this filter reduces a step input to  $1/e \approx 0.37$  of its value after 10 steps, i.e.,  $(0.9)^{10} = 0.35$ , and that 10 steps here corresponds to 1 s with  $T_I = 0.1$  s.)

Comparing Figures 5 and 8, it is seen the phase accumulation results are reduced by a factor of 20.

$$b_{sub\ 1} = T_{sub\ r}/T_{sub\ l} = 0.05$$

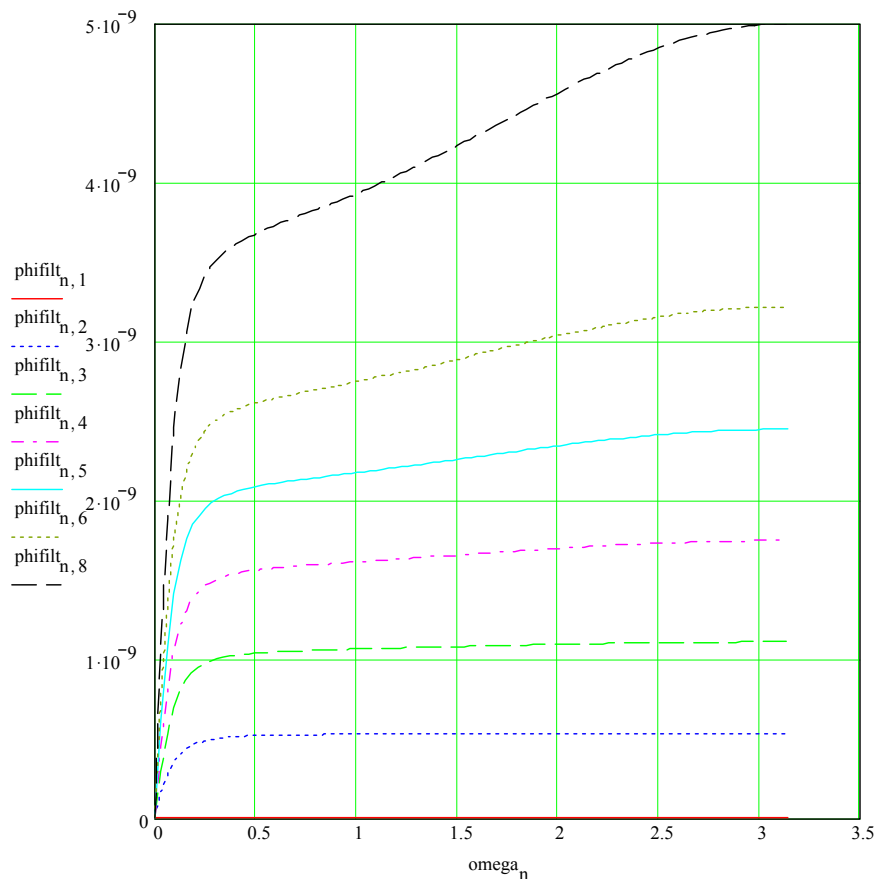


Figure 8. Filtered phase accumulation frequency response magnitude for nodes 2 ( $\phi_{n,1}$ ), 3 ( $\phi_{n,2}$ ), 4 ( $\phi_{n,3}$ ), 5 ( $\phi_{n,4}$ ), 6 ( $\phi_{n,5}$ ), 7 ( $\phi_{n,7}$ ), and 9 ( $\phi_{n,9}$ ), respectively, for  $T_r/T_l = 0.05$ . The filter is an first-order, low-pass filter with equivalent time constant of 1 s.

## 6 Split path syntonization scenario

Reference [8] proposes a scheme that attempts to avoid phase error accumulation in nodes subsequent to the TC where the sinusoidal phase error perturbation is applied, by using the free-running node clock frequencies to compute residence times. However, the corrected master event timestamps based on the unsyntonized TC clocks are used to estimate the frequency offset of each TC relative to the master. This frequency offset estimate is then used to compute the residence time error for that TC. The residence time errors in the successive TCs are accumulated in a separate field, and can be used to correct the phase estimate. A schematic for this scheme, taken from [8], is reproduced in the second and third figures of Appendix IV (for comparison, a schematic for the syntonized TC, also taken from [8], is reproduced in the first figure of Appendix IV).

We now analyze the scheme proposed in [8]. In the notation of section 2 of the current document, the frequency offset of a TC relative to the master,  $\mu_{k,i}$  is measured, but is used only to correct the phase and not the frequency. If we let  $v_{k,i}$  be the actual (i.e., free-running) frequency offset of TC  $k$  relative to the master, then the measured frequency offset at node  $k$  is still given by Eq. (2-4), but now the  $v_{k,i}$  are not adjusted. Expressing the final equation of Eq. (2-4) to  $O(v_{k,i})$  (i.e., neglecting higher order terms, because the frequency offsets are still small compared to 1), we obtain

$$\begin{aligned} \mu_{k,i} &= \frac{v_{k,i-1} - \frac{T_r}{T_l} \sum_{j=1}^{k-1} (v_{j,i} - v_{j,i-1})}{1 + \frac{T_r}{T_l} \sum_{j=1}^{k-1} (v_{j,i} - v_{j,i-1})} \\ &\cong \left[ v_{k,i-1} - \frac{T_r}{T_l} \sum_{j=1}^{k-1} (v_{j,i} - v_{j,i-1}) \right] \left[ 1 - \frac{T_r}{T_l} \sum_{j=1}^{k-1} (v_{j,i} - v_{j,i-1}) \right] \\ &\cong v_{k,i-1} - \frac{T_r}{T_l} \sum_{j=1}^{k-1} (v_{j,i} - v_{j,i-1}) \end{aligned} \quad (6-1)$$

In Eq. (6-1), the perturbation is applied at node 1, which means the frequency offset of node 1 varies with time. The frequency offsets of the other nodes are fixed. Then, in the summation, terms for  $j = 2, 3, \dots, k-1$  vanish, and we obtain

$$\mu_{k,i} = v_{k,i-1} - \frac{T_r}{T_l} (v_{1,i} - v_{1,i-1}). \quad (6-2)$$

The measured frequency offset given by Eq. (6-2) is used to obtain the error in residence time due to lack of syntonization at each respective node. The total error is obtained by accumulating over nodes 2 through  $k$  (see the second figure in Appendix IV, taken from [8]). The resulting cumulative error due to lack of syntonization is

$$T_r \sum_{j=2}^{k-1} \mu_{j,i} = T_r \sum_{j=2}^{k-1} v_{j,i-1} - \frac{T_r^2}{T_l} (k-2) (v_{1,i} - v_{1,i-1}). \quad (6-3)$$

We have omitted the direct contribution from node 1, i.e., the TC where the syntonization is applied, as we did in the previous sections. The contribution from this TC is simply the applied perturbation itself. The desire here is to see the accumulation beyond this quantity.

The actual time the  $i^{\text{th}}$  Sync message arrives at TC  $k$  is (the notation is the same as in section 2)

$$m_{actual,k,i} = m_{0,i} + (k-1)T_r. \quad (6-4)$$

The corrected master time at TC  $k$ , based on free-running clocks used to measure residence time, is

$$m_{k,i} = m_{0,i} + (k-1)T_r + T_r \sum_{j=1}^{k-1} v_{j,i}. \quad (6-5)$$

In Eq. (6-5), the measured frequency offset sum of Eq. (6-3) is used to correct the actual frequency offset sum in the last term of Eq. (6-5); this is done by replacing  $v_{k,i}$  by  $v_{k,i} - \mu_{k,i}$ . The result is (again, omitting the direct contribution from TC 1, where the perturbation is applied)

$$m_{k,i} = m_{0,i} + (k-1)T_r + T_r v_{1,i} + T_r \sum_{j=2}^{k-1} (v_{j,i} - v_{j,i-1}) + \frac{T_r^2}{T_I} (k-2)(v_{1,i} - v_{1,i-1}). \quad (6-6)$$

The first summation in Eq. (6-6) is zero because the frequency offsets for nodes 2 through  $k$  do not vary. Omitting this term and comparing with Eq. (6-4), it is seen that the phase error accumulation is

$$\phi_{k,i} = T_r v_{1,i} + \frac{T_r^2}{T_I} (k-2)(v_{1,i} - v_{1,i-1}). \quad (6-7)$$

The first term is the direct contribution of the perturbation; as noted above, we ignore this term because we are interested in the amount that the phase error accumulates beyond this term. Inserting a sinusoidal frequency variation as in Eq. (3-1) and noting that the equivalent sinusoidal phase variation amplitude is  $B = AT_r$  (see section 4), we obtain for the phase error accumulation

$$\phi_{k,i} = B \frac{T_r}{T_I} (k-2)(1 - e^{-j\omega})e^{j\alpha}. \quad (6-8)$$

The magnitude of the phase error accumulation frequency response is (using Eq. (3-7))

$$|\phi_{k,i}| = B \frac{T_r}{T_I} (k-2) \sqrt{2(1 - \cos \omega)}. \quad (6-9)$$

The maximum amplitude of the phase error accumulation occurs for  $\omega = \pi$ , i.e., period equal to twice the frequency update interval. The result is

$$|\phi_{k,i}|_{\max} = 2B \frac{T_r}{T_I} (k-2). \quad (6-10)$$

The corresponding result for the case of syntonized TCs is given by Eq. (4-6) with  $\omega = \pi$ , i.e.

$$|\phi_{k,i}|_{\max} = B \cdot \left[ \left( 1 + 2 \frac{T_r}{T_l} \right)^{k-2} - 1 \right]. \quad (6-11)$$

Comparing these results, it is seen that Eq. (6-11) reduces to Eq. (6-10) for  $T_r \ll T_l$ , but Eq. (6-11) can exceed Eq. (6-10) by a large margin when  $T_r$  is appreciable compared to  $T_l$ . Figure 9 plots the ratio of the accumulation factor of Eq. (6-11) to the accumulation factor of Eq. (6-10), i.e.,

$$F = \frac{\left( 1 + 2 \frac{T_r}{T_l} \right)^{k-2} - 1}{2(k-2) \frac{T_r}{T_l}} \quad (6-12)$$

for various values of  $k$  and  $T_r / T_l$ .

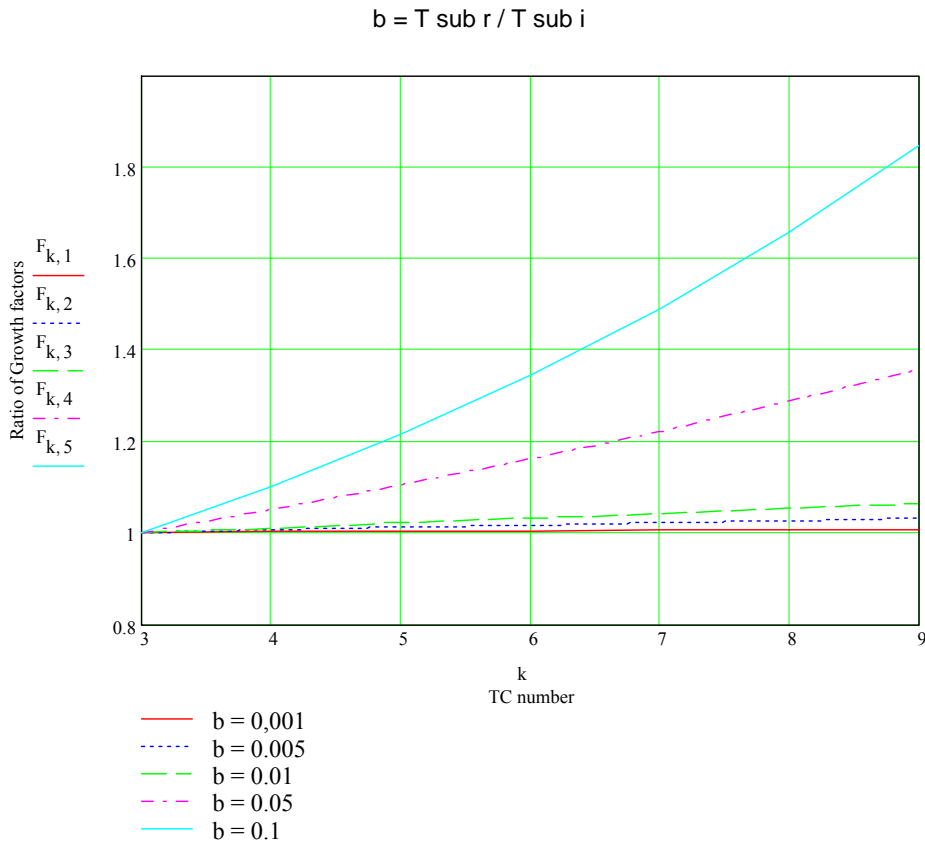


Figure 9. Plot of ratio of growth factors for phase accumulation for syntonized TC chain to phase accumulation for unsyntonized TC chain.

## 7 Conclusions

The analysis shows that if  $T_r \ll T_I$ , a very large number of hops is required before the effect of a frequency offset perturbation on downstream accumulates to the level of the perturbation. For example, for residence time on the order of 0.001 of the frequency update interval, the frequency offset amplitude due to the applied perturbation after 100 hops is 0.2% of the applied perturbation amplitude. For AVB networks, where it is likely that  $T_r/T_I = 0.1$  in very worst case, the frequency offset accumulates to the level of the perturbation after 11 hops. After 7 hops, the frequency offset is approximately half the level of the applied perturbation. The phase offset also accumulates slowly when residence time is small compared to frequency update interval, though the accumulation is faster than for the frequency offset accumulation (e.g., for residence time on the order of 0.001 of the frequency update interval, the phase offset amplitude due to the applied perturbation after 100 hops is 0.21 of the applied perturbation amplitude). For AVB networks, where residence time could be as large as one-tenth the frequency update interval, the phase accumulation is about twice the applied perturbation amplitude after 7 hops. A scheme (see [8]) that does not syntonize the TCs but uses the measured frequency offset relative to the master to adjust the phase was also investigated. Here, the phase accumulation due to a sinusoidal phase perturbation is slower than in the syntonized chain case, though the results are almost indistinguishable for small ratios of residence time to frequency update interval, even for a very large number of hops (e.g., for residence time on the order of 0.001 of the frequency update interval, the phase offset amplitude due to the applied perturbation after 100 hops is 0.2 of the applied perturbation amplitude). For AVB networks, where residence time could be as large as one-tenth the frequency update interval, the phase accumulation is about 1.2 times the applied perturbation amplitude after 7 hops.

In addition, if 802.1AS networks must tolerate sinusoidal phase wander in the clocks, consideration should be given to the level of wander that must be tolerated and the desired performance. The examples here used 100 ns sinusoidal wander amplitude; this was taken from [6], but no justification was given (either in [6] or here) for this level. It should be noted that the phase error accumulation results in section 4 are unfiltered; section 5 shows an example of the reduction that results after endpoint filtering.

It may be asked why the frequency offset downstream of a perturbation should not be at least at the level of the perturbation itself. The reason is that any given TC is still syntonizing to the master. The frequency offset at an intermediate TC affects only the residence time measurement. Furthermore, the frequency offset measured at a particular TC is impacted only to the extent that successive residence times at upstream TCs *are different* (by successive, we mean at successive frequency update times). If intermediate residence times are in error but did not vary, the syntonization of a downstream TC would not be affected (though the time synchronization of the system would most definitely be affected).

## 8 References

- [1] Chuck Harrison, *Email to P1588 Reflector*, February 18, 2007.
- [2] Chuck Harrison, *Email to P1588 Reflector*, February 22, 2007.
- [3] E. L. Varma and J. Wu, *Analysis of Jitter Accumulation in a Chain of Digital Regenerators*, Proceedings of IEEE Globecom, Vol. 2, pp. 653 – 657, 1982.
- [4] ITU-T Rec. G.8251, *The Control of Jitter and Wander within the Optical Transport Network*, ITU-T, Geneva, November, 2001 (Amendment 1, June, 2002, Corrigendum 1, June, 2002).

- [5] IEEE P1588™/D1-A 17 February 2007, *Draft Standard for a Precision Clock Synchronization Protocol for Networked Measurement and Control Systems*, Draft D1-A, February 17, 2007.
- [6] Chuck Harrison, *Cascaded Gain Phenomena in IEEE 1588v2 Transparent Clock Chains: an Initial Study*, contribution distributed to IEEE 1588 and IEEE 802.1, February 28, 2007.
- [7] Geoffrey M. Garner, *Analysis of Clock Synchronization Approaches for Residential Ethernet*, presentation to IEEE 802.3 Residential Ethernet SG, San Jose, September, 2005.
- [8] Chuck Harrison, *Transparent Clock Gain Cascade: Split Path Scenario*, contribution distributed to IEEE 802.1, March 9, 2007.

Appendix I. Mathcad listing and plots for frequency offset accumulation results.

$k := 1..9$        $p := 1..5$   
 $b_1 := 0.001$        $b_2 := 0.005$        $b_3 := 0.01$

$b_4 := 0.05$        $b_5 := 0.1$

$M := 100$

$n := 0..M$

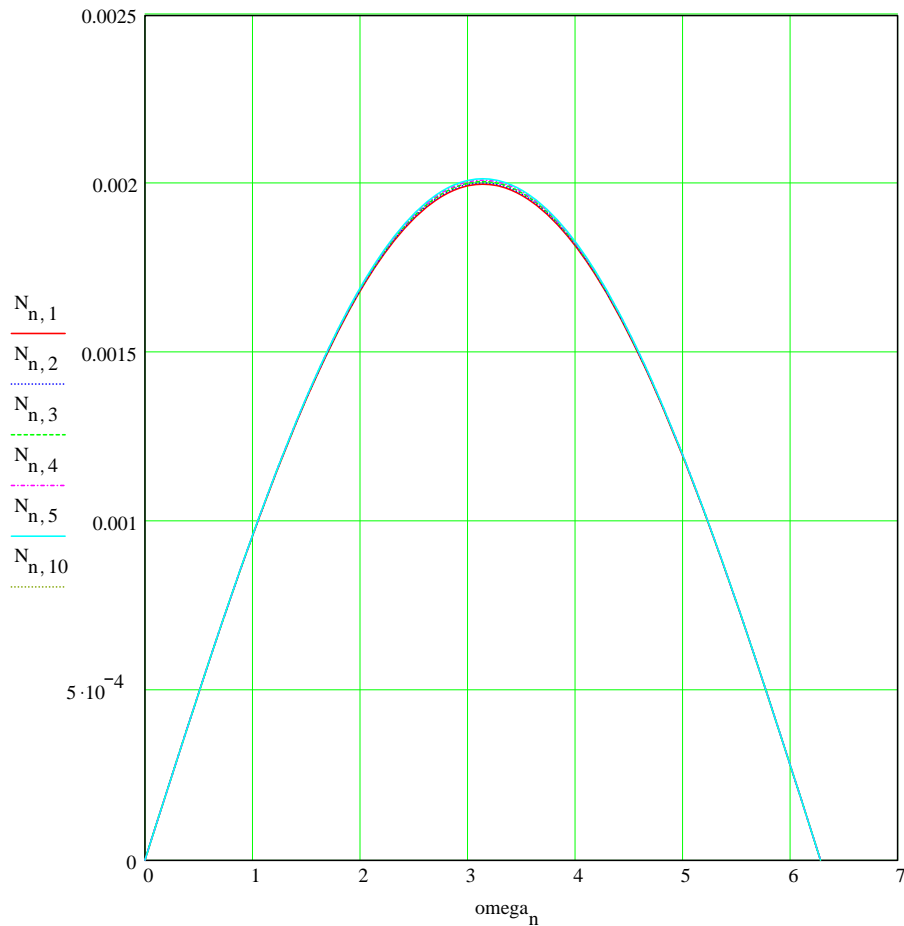
$K_k := k + 1$

$$\omega_n := \frac{(2 \cdot \pi \cdot n)}{M}$$

GM = node 0  
 perturbation applied at node 1  
 $K_{sub\ k}$  = node index ( $k = 1$  corresponds to node 2 (i.e., first node after node where perturbation is applied))  
 $N_{sub\ n,k}$  = magnitude of frequency response ( $n$  = frequency index,  $k$  = node number index)

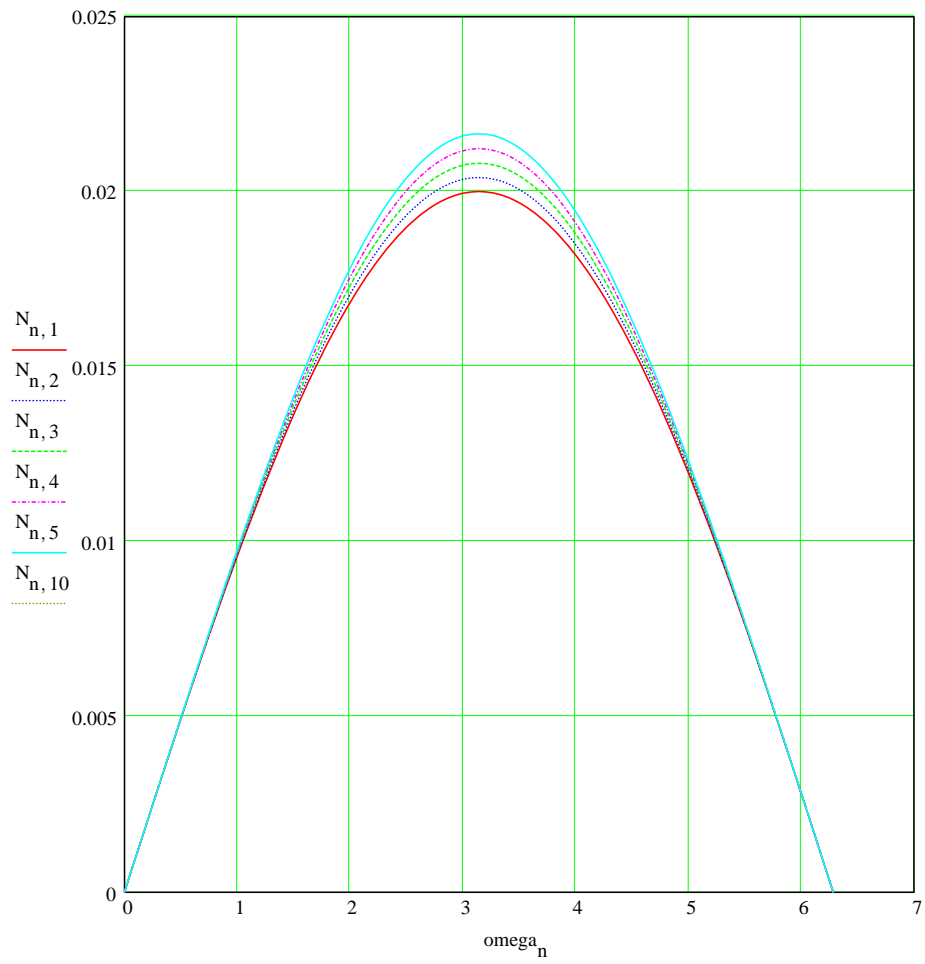
$$N_{n,k} := \sqrt{\left[ (b_1)^2 \cdot 2 \cdot (1 - \cos(\omega_n)) \right] \cdot \left[ (1 + 2 \cdot b_1 \cdot (1 + b_1) \cdot (1 - \cos(\omega_n))) \right]^{K_k - 2}}$$

$b_{sub\ 1} = T_{sub\ r} / T_{sub\ l} = 0.001$



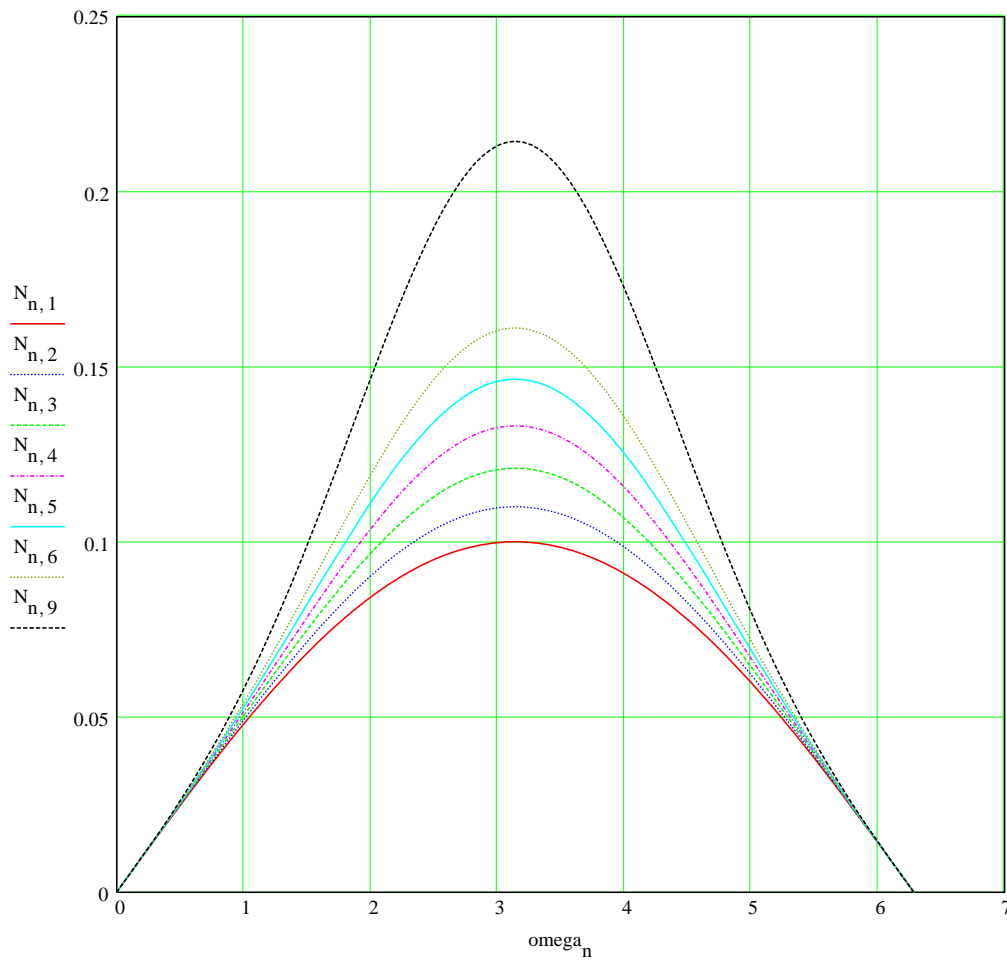
$$N_{n,k} := \sqrt{\left[ (b_3)^2 \cdot 2 \cdot (1 - \cos(\omega_n)) \right] \cdot \left[ (1 + 2 \cdot b_3 \cdot (1 + b_3)) \cdot (1 - \cos(\omega_n)) \right]^{k-2}}$$

$b_3 = T_r / T_l = 0.01$



$$N_{n,k} := \sqrt{\left[ (b_4)^2 \cdot 2 \cdot (1 - \cos(\omega_n)) \right] \cdot \left[ (1 + 2 \cdot b_4 \cdot (1 + b_4) \cdot (1 - \cos(\omega_n))) \right]^{k-2}}$$

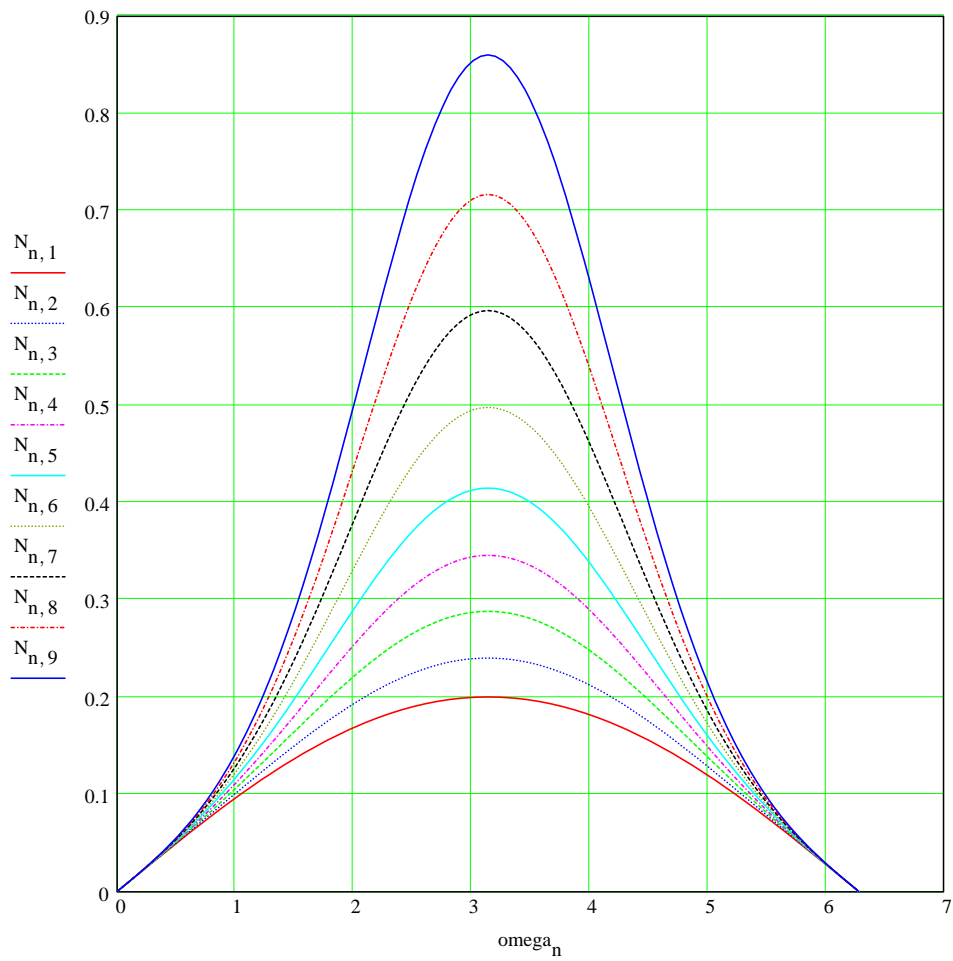
$$b_4 = T_r / T_l = 0.05$$



$$N_{n,k} := \sqrt{\left[ (b_5)^2 \cdot 2 \cdot (1 - \cos(\omega_n)) \right] \cdot \left[ (1 + 2 \cdot b_5 \cdot (1 + b_5) \cdot (1 - \cos(\omega_n))) \right]^{k-2}}$$

$$N_{50,9} = 0.86$$

$$b_5 = T_{r/T_l} = 0.1$$



Appendix II. Mathcad listing and plots for phase error accumulation results.

$k := 1..9$        $p := 1..5$   
 $b_1 := 0.001$        $b_2 := 0.005$        $b_3 := 0.01$

$b_4 := 0.05$        $b_5 := 0.1$

$M := 100$

$n := 0..M$

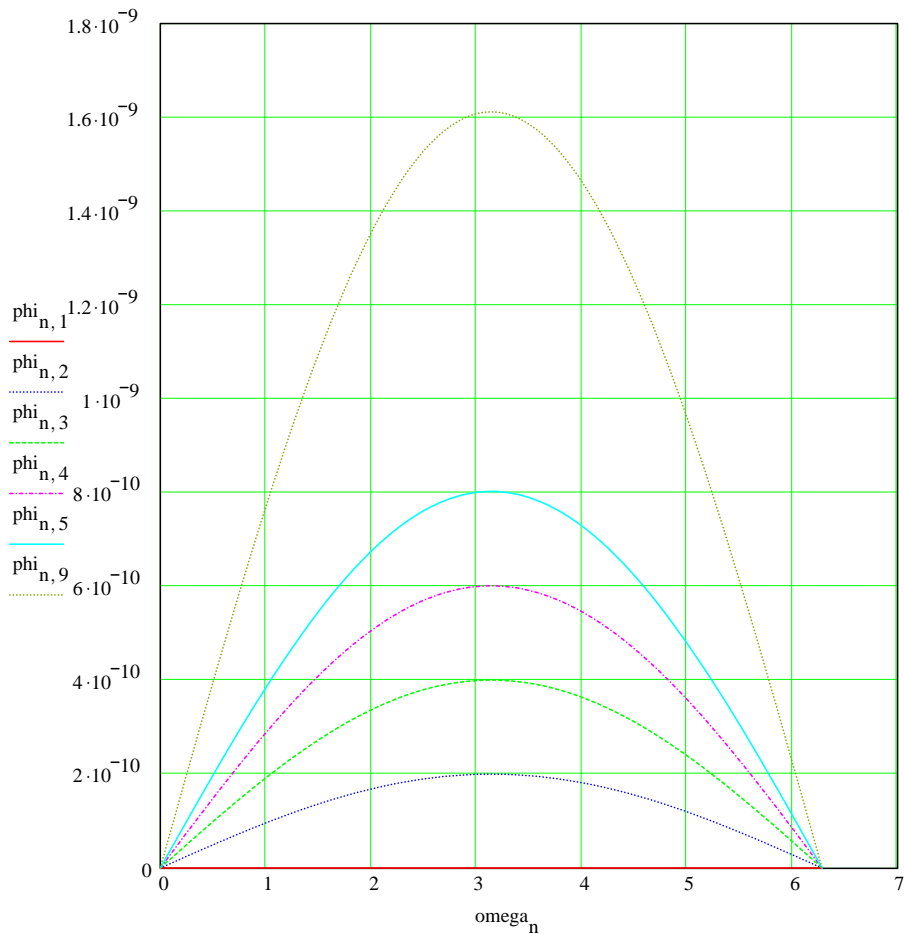
$K_k := k + 1$

$$\omega_n := \frac{(2 \cdot \pi \cdot n)}{M}$$

$$\phi_{n,k} := B \cdot \left| \left( 1 + b_1 - b_1 \cdot e^{-i \cdot \omega_n} \right)^{K_k - 2} - 1 \right|$$

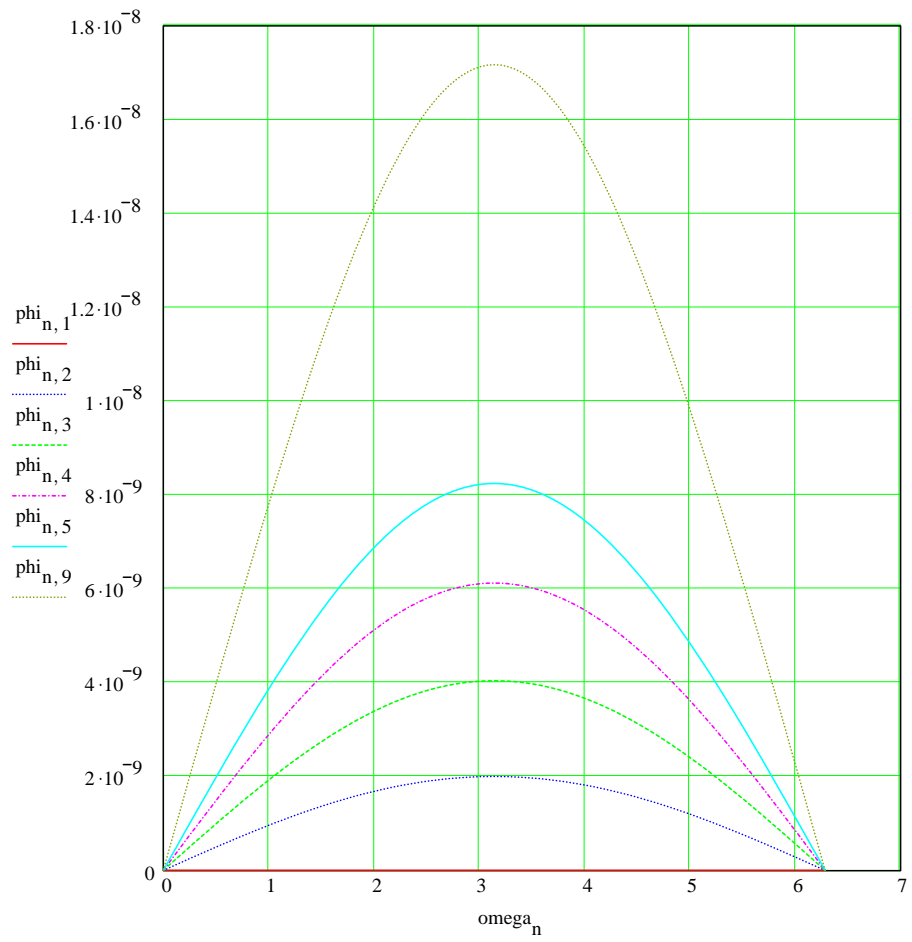
GM = node 0  
 perturbation applied at node 1  
 $K_{sub k}$  = node index ( $k = 1$  corresponds to node 2 (i.e., first node after node where perturbation is applied))  
 $N_{sub n,k}$  = magnitude of frequency response ( $n$  = frequency index,  $k$  = node number index)

$b_{sub 1} = T_{sub r} / T_{sub l} = 0.001$



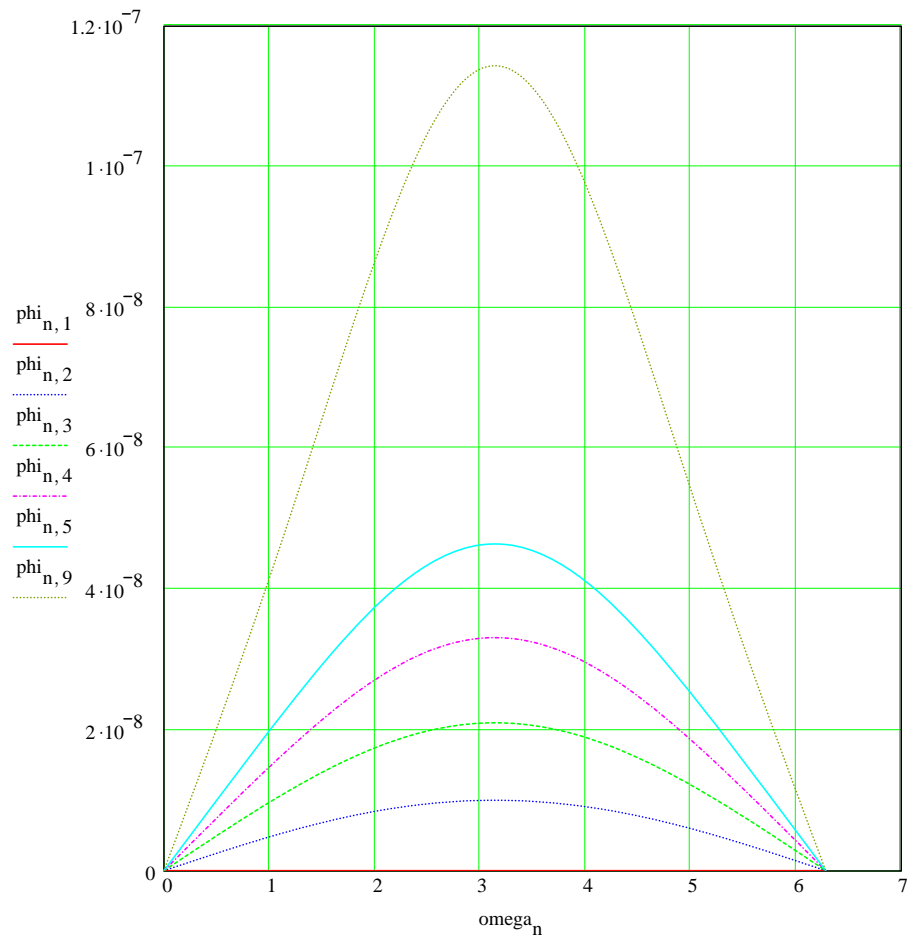
$$\phi_{n,k} := B \cdot \left| \left( 1 + b_3 - b_3 \cdot e^{-i \cdot \omega_n} \right)^{K_k - 2} - 1 \right|$$

$b_1 = T \cdot r / T \cdot l = 0.01$



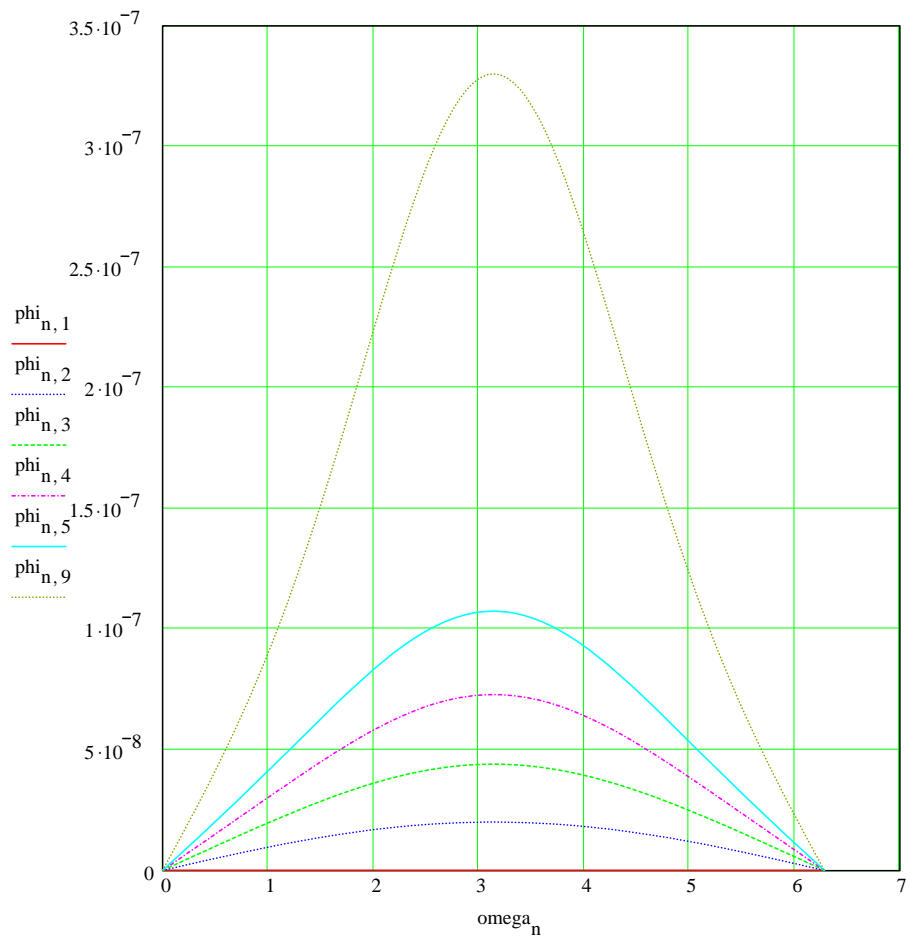
$$\text{phi}_{n,k} := B \cdot \left| \left( 1 + b_4 - b_4 \cdot e^{-i \cdot \text{omega}_n} \right)^{K_k - 2} - 1 \right|$$

b sub 1 = T sub r/T sub l = 0.05



$$\text{phi}_{n,k} := B \cdot \left| \left( 1 + b_5 - b_5 \cdot e^{-i \cdot \text{omega}_n} \right)^{K_k - 2} - 1 \right|$$

b sub 1 = T sub r/T sub l = 0.1



Appendix III. Modification listing from [6] to obtain phase error time history at TC 3, for perturbation period equal to 3.1 times the frequency update interval.

$\text{msec} := 10^{-3}$        $\text{nsec} := 10^{-9}$   
 $\text{simsteps} := 150$        $i := 0 .. \text{simsteps} - 1$

$\text{syncperiod} := 10 \cdot \text{msec}$   
 $\text{syntonizedsteps} := 10$

$\text{residencetime} := 5 \cdot \text{msec}$        $\text{cableDelay} := 10 \cdot \text{nsec}$

$\text{testperiod} := 3.1 \cdot \text{syntonizedsteps} \cdot \text{syncperiod}$        $\text{testamplitude} := 100 \cdot \text{nsec}$

$\text{issuetime}_i := i \cdot \text{syncperiod}$

$\text{SyncArrival}_i := \text{issuetime}_i + 5 \cdot \text{msec} + 2 \cdot \text{cableDelay}$

$\text{NodeClockOffset} := 0.5$

$\text{SEIT}_i := \text{SyncArrival}_i + \text{NodeClockOffset}$   
 $\text{preciseOriginTimestamp}_i := \text{issuetime}_i$   
 $\text{meanpathdelay} := \text{cableDelay}$

$\text{testdeviation}_i := \text{testamplitude} \cdot \sin \left[ (2) \cdot \pi \cdot i \cdot \frac{\text{syncperiod}}{\text{testperiod}} \right]$

$\text{follow\_upCorrectionField}_i := 5 \cdot \text{msec} + \text{cableDelay} + \text{testdeviation}_i$

$\text{CMET}_i := \text{preciseOriginTimestamp}_i + \text{meanpathdelay} + \text{follow\_upCorrectionField}_i$

$\text{integrationstart}_i := \text{syntonizedsteps} \cdot \left( \text{floor} \left( \frac{i}{\text{syntonizedsteps}} + 0.001 \right) - 1 \right)$

$\text{syntonizedrate}_i := \begin{cases} 1 & \text{if } i < \text{syntonizedsteps} \\ \frac{\text{CMET}_{(\text{integrationstart}_i + \text{syntonizedsteps})} - \text{CMET}_{(\text{integrationstart}_i)}}{\text{SEIT}_{(\text{integrationstart}_i + \text{syntonizedsteps})} - \text{SEIT}_{(\text{integrationstart}_i)}} & \text{otherwise} \end{cases}$

$\text{residencecorrection}_i := \text{residencetime} \cdot \text{syntonizedrate}_i$

$\text{idealoutputtime}_i := \text{SyncArrival}_i + \text{residencetime}$

$\text{outputFollow\_upCorrectionField}_i := \text{follow\_upCorrectionField}_i + \text{meanpathdelay} + \text{residencecorrection}_i$

$\text{outputFollow\_upPreciseOriginTimestamp}_i := \text{preciseOriginTimestamp}_i$

$\text{effectiveOutputtime}_i := \text{outputFollow\_upCorrectionField}_i + \text{outputFollow\_upPreciseOriginTimestamp}_i$

$\text{outputdeviation}_i := \text{effectiveOutputtime}_i - \text{idealoutputtime}_i$

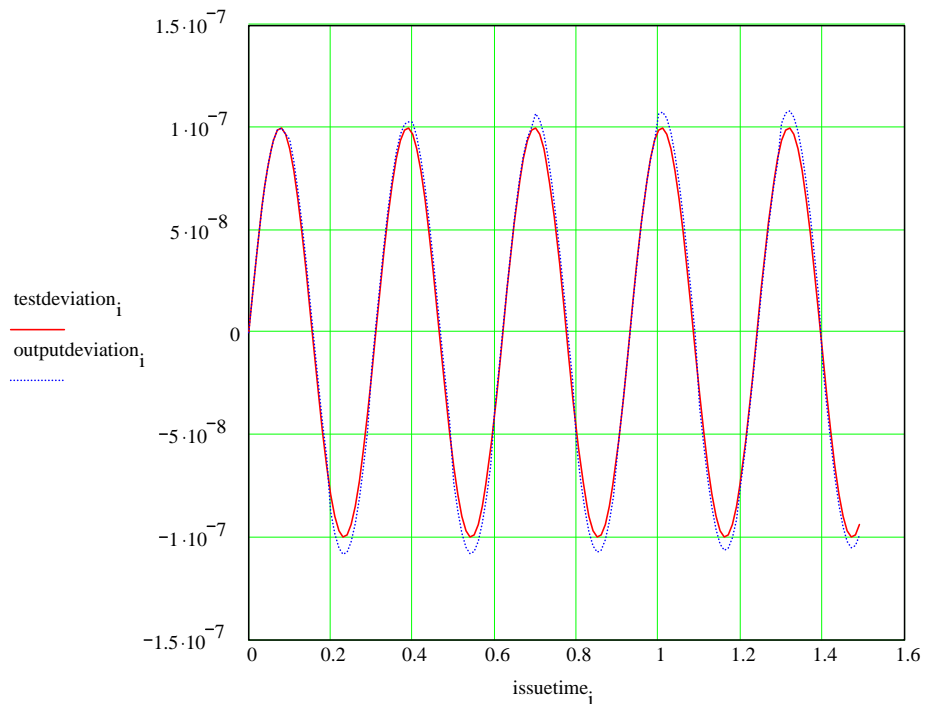
$$\text{rmsinputdeviation} := \left[ \frac{1}{\text{simsteps}} \cdot \sum_i (\text{testdeviation}_i)^2 \right]^{\frac{1}{2}} \quad \text{rmsinputdeviation} = 7.105 \cdot 10^{-8}$$

$$\text{rmsoutputdeviation} := \left[ \frac{1}{\text{simsteps}} \cdot \sum_i (\text{outputdeviation}_i)^2 \right]^{\frac{1}{2}} \quad \text{rmsoutputdeviation} = 7.557 \cdot 10^{-8}$$

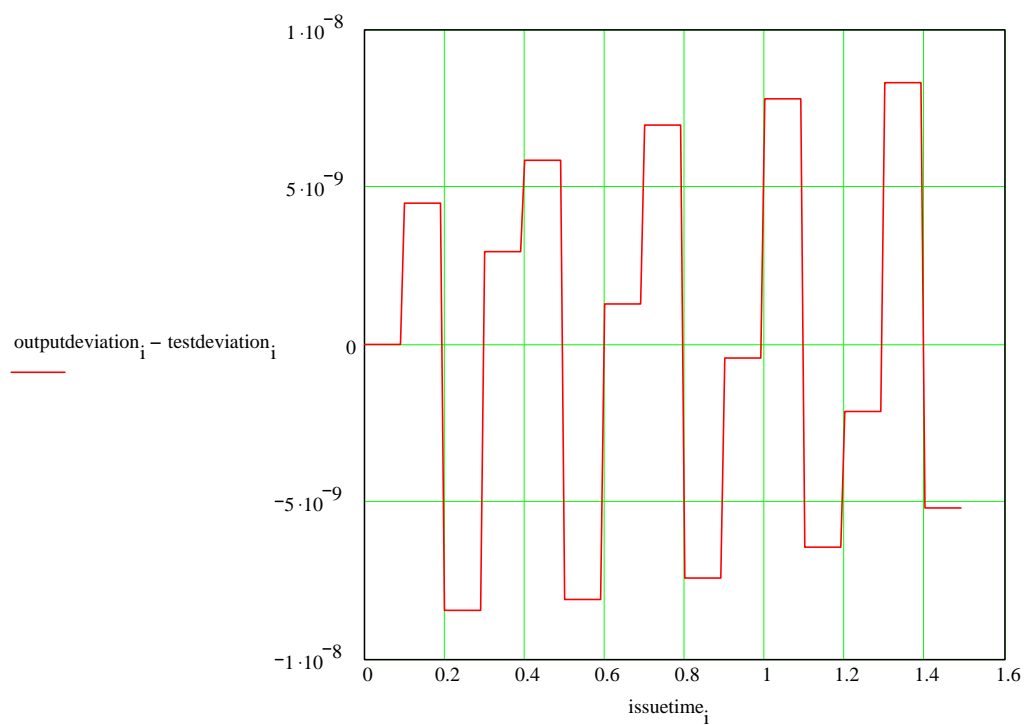
$$\text{gainpeaking} := \frac{\text{rmsoutputdeviation}}{\text{rmsinputdeviation}}$$

$$\text{gainpeaking} = 1.064$$

$$20 \cdot \log(\text{gainpeaking}) = 0.535$$



T sub r/Tsub l = 0.05



Appendix IV. Figures of reference [8].

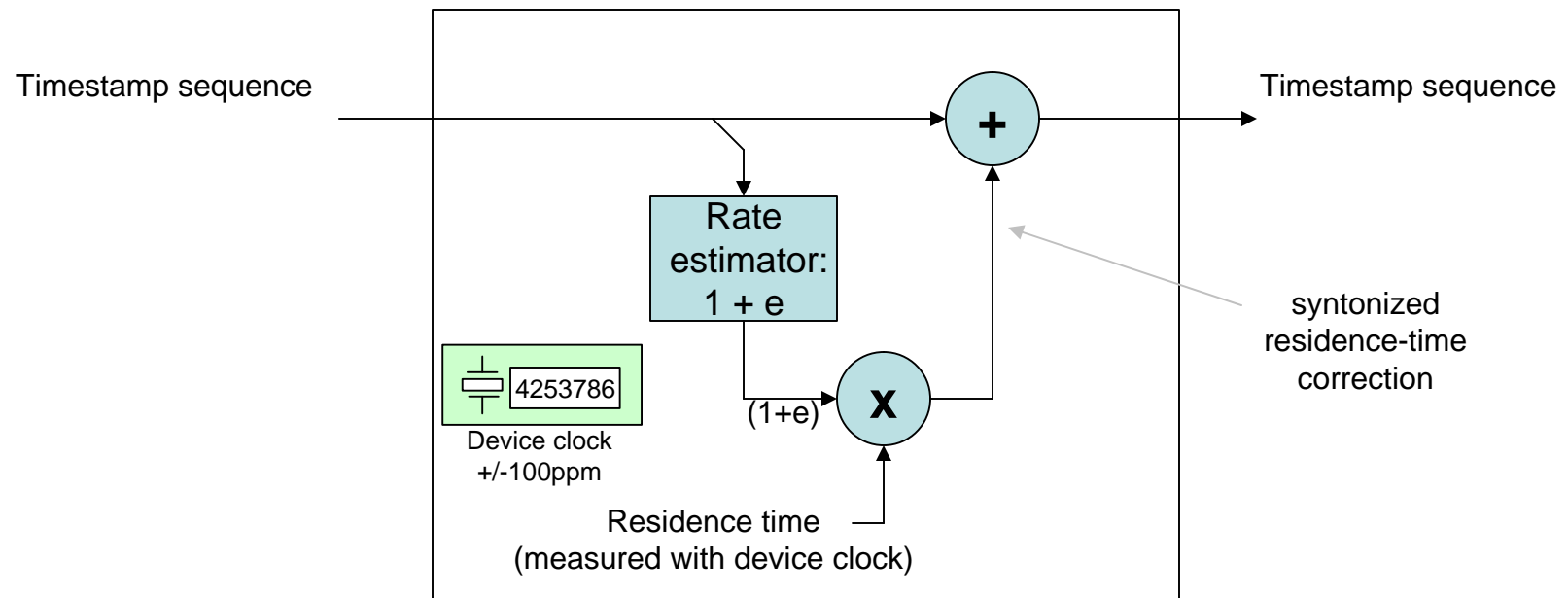
# Transparent Clock Gain Cascade: Split-path scenario

802.1AS Precision Timing

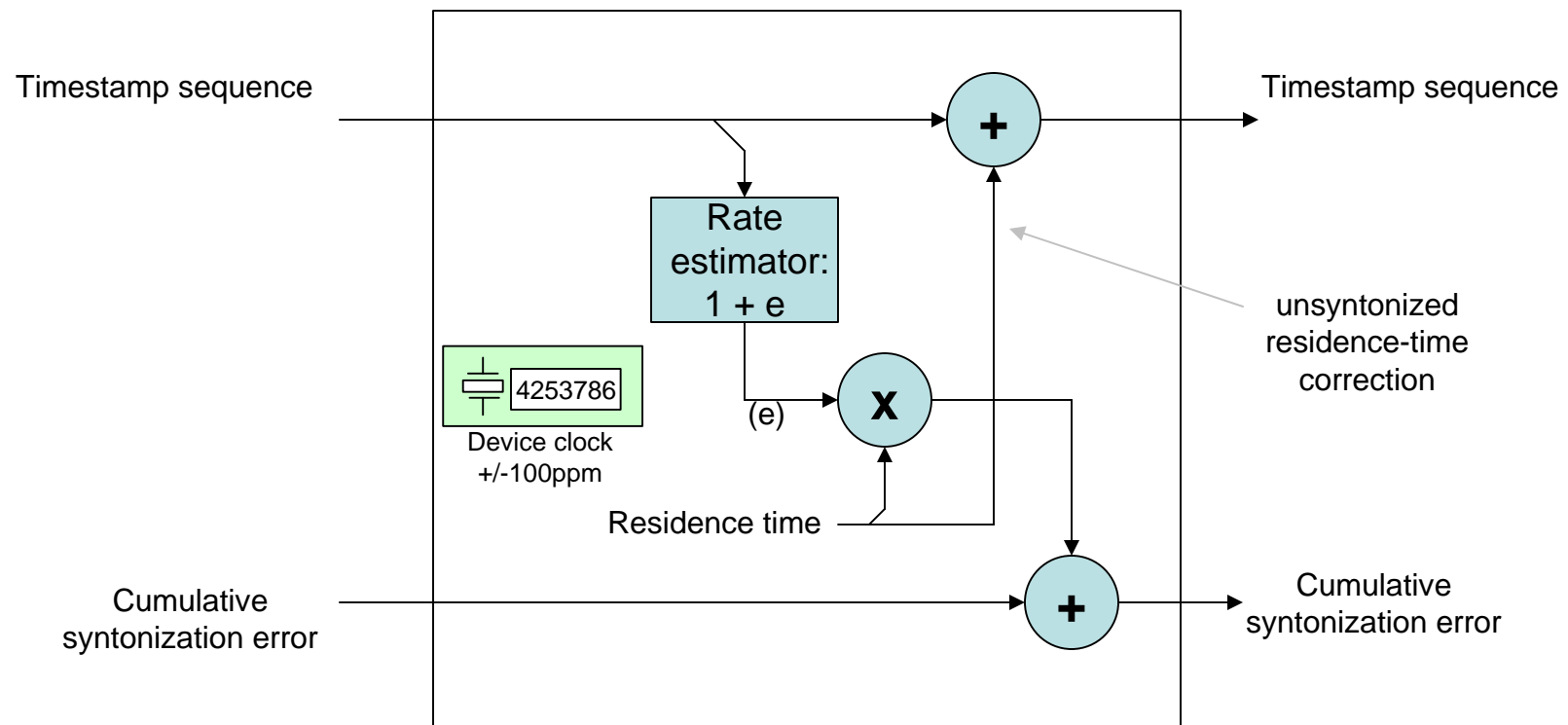
9 March 2007

Chuck Harrison

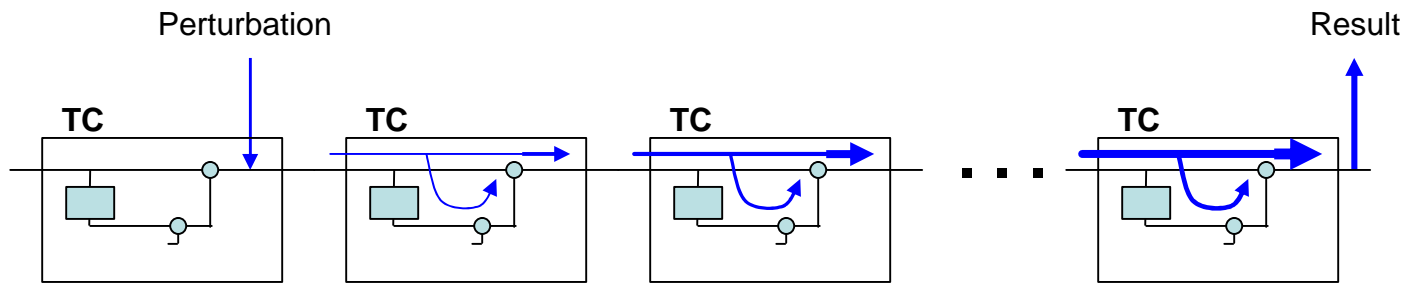
# Syntonized TC model



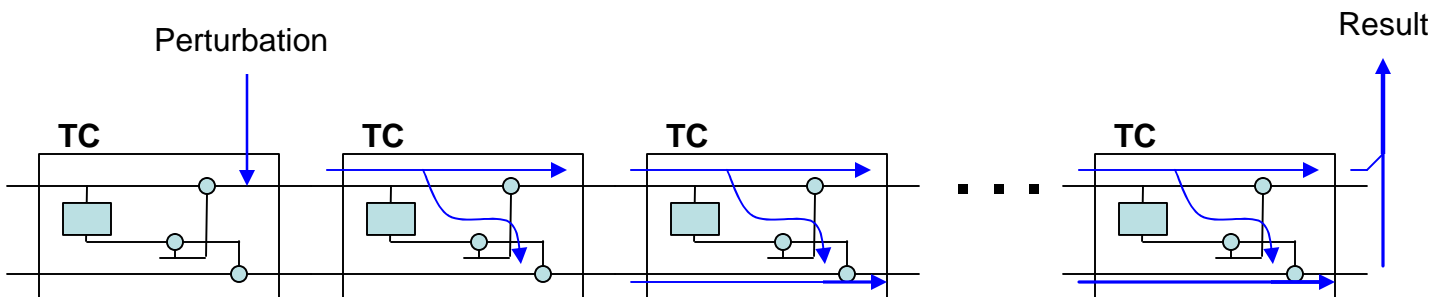
# Split-path Synchronized TC model



# Breaking the syntonization cascade



*Gain cascade effect*



*Error summation effect*